Title
In Vitro-Reconstituted Virus-like-particle Delivery of Self-Amplifying RNA Genes

Author
Biddlecome, Adam Min

Publication Date
2019

Peer reviewed|Thesis/dissertation

UNIVERSITY OF CALIFORNIA

Los Angeles

In Vitro-Reconstituted Virus-like-particle Delivery of Self-Amplifying RNA Genes

A dissertation submitted in partial satisfaction of the requirements for the degree Doctor of Philosophy in Biochemistry, Molecular, and Structural Biology

by

Adam Min Biddlecome

2019

ABSTRACT OF THE DISSERTATION

In Vitro-Reconstituted Virus-like-particle Delivery

of Self-Amplifying RNA Genes

by

Adam Min Biddlecome

Doctor of Philosophy in Biochemistry, Molecular, and Structural Biology

University of California, Los Angeles, 2019

Professor William M. Gelbart, Chair

The delivery of RNA genes has great potential in a range of therapeutic applications. A couple of main limitations for RNA-based therapies include its vulnerability to ribonuclease (RNase) digestion, and its transient and low expression levels due to its lack of amplification. Accordingly, a gene delivery platform that includes *self-amplifying* mRNA inside a *protective* capsid allowing for cell targeting and uptake could represent a major step forward in mRNA-based gene therapy.

The self-amplifying nature of viral-encoded RNA-dependent RNA polymerases (RdRp) of *Nodamura virus* holds promise in the development of a platform for self-amplifying RNA gene delivery. To protect and assist in uptake of mRNA encoding an RdRp coupled to a gene of interest, plant virus-like-particles (VLPs) are a strong candidate. Cowpea chlorotic mottle virus

(CCMV) capsid protein has been shown to be able to package in vitro heterologous mRNAs, and also to make the genes available to mammalian cells. To better characterize the uptake and amplification in mammalian cells of RdRp-associated genes (also called a replicon, because of its self-amplifying nature), both when naked or encapsidated, reporter genes such as enhanced yellow fluorescent protein (EYFP) or luciferase were used.

In collaboration with the German pharmaceutical company Boehringer Ingelheim (B-I), evaluation of possible efficacy of this platform for a cancer vaccine was explored by incorporation of a model antigen (Ovalbumin epitope, SIINFEKL) sequence into the RNA1 of *Nodamura virus*. From *in vitro* studies involving incubation of OVA-replicon-VLPs, we observed that CCMV VLPs can be taken up by dendritic cells, where replication then occurs to promote increased production of antigen. Flow cytometry analysis revealed increased expression of maturation markers, and assaying the dendritic cell content by qPCR showed a significant number of SIINFEKL epitope-containing RNA. After these OVA-replicon-VLPs are injected into mice, a population of SIINFEKL-specific CD8+ (cytotoxic) T cells results.

The dissertation of Adam Min Biddlecome is approved.

Catherine F. Clarke

Feng Guo

William M. Gelbart, Committee Chair

University of California, Los Angeles

2019

Dedication

To my family and loved ones, for all the encouragement.

Table of Contents

List of Figures

Acknowledgements

I would like to thank Professors William M. Gelbart and Charles M. Knobler for their constant guidance during this phase of my academic journey. They have a true passion for science, and genuine concern for the members of their research group. I would also like to thank all the friends and Gelbart/Knobler group members who I've met at UCLA.

Chapter 2 owes special thanks to Dr Leonid Gitlin, formerly of the group of Dr Raul Andino at University of California, San Francisco. They provided the initial *Nodamura virus* replicon construct from which were derived many of the constructs used throughout this work, as well as helpful advice. Some of the cell culture and molecular biology techniques were learned from Dr Odisse Azizgolshoni and Dr Devin Brandt, respectively. The dose dependence of the replicon was also investigated by Cheylene Tanimoto, Abby Thurm, and Dr Devin Brandt – they primarily used a fluorescent gene for their studies.

Chapter 3 is a version of Biddlecome A, Habte HH, McGrath KM, Sambanthamoorthy S, Wurm M, Sykora MM, Knobler CM, Lorenz IC, Lasaro M, Elbers K, Gelbart WM. (2019) Delivery of self-amplifying RNA vaccines in in vitro reconstituted virus-like particles. PLoS ONE 14(6): e0215031.

The work in chapter 3 represents a significant amount of teamwork between UCLA and Boehringer Ingelheim's US headquarters in Ridgefield, Connecticut for *in vitro* dendritic cell experiments. Dr Knut Elbers has been the lead on Boehringer Ingelheim's side of the collaboration, while Dr William Gelbart and Dr Charles Knobler led on the side of UCLA. Dr Ivo Lorenz was helpful in early planning of the work in this paper. While I spent almost two

months as an intern learning and executing some of the experiments in this paper, Dr Marcio Lasaro oversaw the experimental direction for the dendritic cell experiments. Dr Habtom Habte was in charge of the experiments. Katherine McGrath was in charge of RNA quantification and associated molecular biology. Sharmila Sambanthamoorthy performed the flow cytometry. For the *in vivo* work, I prepared the reagents, but the vaccinations were overseen by Dr Melanie Wurm in Boehringer Ingelheim's Vienna, Austria location. Analysis of samples were performed by Martina Sykora.

Chapters 4 and 5 involved some help from members, past and present, from the Gelbart/Knobler group. I had helpful discussions with Dr Rees Garmann in planning experiments for a two-molecule replicon strategy. For the cysteine-mutant CCMV, Dr Garmann was again helpful in the process of transfecting and purification of cysteine-CCMV. Dr Christian Beren helped with the gold-labeling of cysteine-CCMV and subsequent electron micrograph imaging. Richard Sportsman helped with the experiment in figure 19 showing mixed assembly of wild type and cysteine CCMV capsid protein. Throughout this work, Richard Sportsman and Dr Christian Beren performed electron microscopy on virus-like particles to confirm successful assembly of various replicon molecules.

Vita

Undergraduate Researcher with Professor Ann Feeney, The Scripps Research Institution, 2010

Research Intern at Neurocrine Biosciences with Dr**.** Jacek Slon-Usakiewicz, 2011-2012

B.S. Bioengineering: Biotechnology, University of California, San Diego 2012

Teaching Assistant in Department of Chemistry and Biochemistry, University of California, Los Angeles 2013-2016

Publication

Biddlecome A, Habte HH, McGrath KM, Sambanthamoorthy S, Wurm M, Sykora MM, Knobler CM, Lorenz IC, Lasaro M, Elbers K, Gelbart WM. (2019) Delivery of self-amplifying RNA vaccines in in vitro reconstituted virus-like particles. PLoS ONE 14(6): e0215031.

Poster Presentation

Adam Biddlecome, Habtom Habte, Charles M. Knobler and William M. Gelbart (2017). Virus-like-particle delivery of Self-amplifying RNA genes. Presented at Seaborg Symposium, University of California, Los Angeles.

Chapter 1: Introduction

The delivery of RNA genes has great potential in a range of therapeutic applications. Nearly any sequence of mRNA can be generated at a reasonable cost, whether it be encoding natural or *de novo* proteins. Compared to DNA gene delivery, mRNA has the advantage that there is no nuclear localization and thus no possibility of genomic integration[Islam 2015]. Some disadvantages it poses for gene delivery include its vulnerability to ribonuclease (RNase) digestion and its capability to elicit innate immune responses[Schott 2010]. Another limitation for *in vivo* applications is that gene expression in cells does not have any amplification, resulting in only transient and low expression levels.

Accordingly, a novel gene delivery platform that includes *self-amplifying* mRNA inside of a protective capsid could represent a major step forward in mRNA-based gene therapy. We address these issues by using viral replicons (self-replicating RNA molecules) for the self-amplification, and self-assembled virus-like particles (VLPs) for the protection, specifically using the RNA-dependent RNA polymerase (RdRp) from *Nodamura virus* (NoV) and capsid protein (CP) from *Cowpea Chlorotic Mottle virus* (CCMV). The CCMV CP is particularly well-suited to package a replicon because it has been shown to package *in vitro* any heterologous RNA that is not much longer than the length of the wild type (WT) genome[Cadena-Nava 2012]. *Nodamura virus* has an RdRp of about 3000 nt, suitable for packaging by this plant CP because it is close in length to CCMV's genomic RNA. Although it is an insect virus, Nodamura is known to be functional in mammalian cells[Garrett 1992].

NoV is a positive-sense RNA virus with a bipartite genome that is co-packaged in the same virion. Similar to CCMV, the capsid has 180 copies of a single capsid protein and a

diameter of around 30 nanometers. NoV is part of the *Nodaviridae* family viruses, which includes the *betanodavirus* genus with fish as the natural host, and *alphanodavirus* genus whose hosts includes various insects, mammals, and fish. NoV (part of the *alphanodavirus* genus) was the first species of the *Nodaviridae* family discovered, and owes its name to the Japanese village of Nodamura, Iwate Prefecture where it was first isolated from *Culex tritaeniorhynchus* mosquitoes[Tesh 1980]. From infected mosquitoes, NoV can be transmitted to cause disease in suckling mice. Furthermore, it causes paralysis and death in suckling mice and hamsters when injected, but no disease in adult animals. In insect hosts, NoV causes stunting, paralysis, and death[Owens 2012].

Figure 1 depicts the viral life-cycle of NoV. This positive-sense genome consists of two RNA molecules, the larger of which includes the RNA1 (3204 nt) gene that encodes for the RdRp, and a subgenomic RNA3 (1336 nt) that encodes for the B2 protein that suppresses host cell RNA interference[Gant 2014]. The other molecule is the RNA2 that encodes for the capsid protein. Studies on NoV and closely related *Flock House virus* (FHV) have elucidated much about the viral lifecycle, including the mechanism by which their RdRps self-amplify their own genes. Upon entering the cell, the cytosolic path to replication begins with translation of the RdRp (also referred to as protein A). The RdRp then binds to the 3' end of RNA1 and generates a complementary minus strand. This double-stranded intermediate can then undergo replication by synthesis of a full positive strand from the minus stand. Another possibility is transcription of a positive-sense subgenomic RNA3 which encodes for proteins B1 and B2. While protein B2 is known to be an RNA silencing suppressor, even shown in certain mammalian cell lines to enhance RNA accumulation[Johnson 2004], protein B1 is of unknown function. RNA2, also a positive-sense and directly translatable RNA, has untranslated regions that promote its own

replication by the RdRp. The full capsid protein alpha assembles around each copy of RNA1 and RNA2, where capsid protein alpha undergoes cleavage prior to cell entry to capsid protein beta (the mature capsid protein) and gamma (responsible for breaching the host cell membrane)[Banerjee 2008]. In addition to replicating in natural hosts such as Drosophila cells, NoV has been shown to also have strong RdRp-dependent replication in mammalian cells[Garrett 1992]. Further, it has been demonstrated that – not only its own genes - but also any gene of interest can be amplified if inserted into the subgenomic region of RNA1 directly after the RdRp open reading frame and before the 3' untranslated region (UTR)[Gitlin 2014].

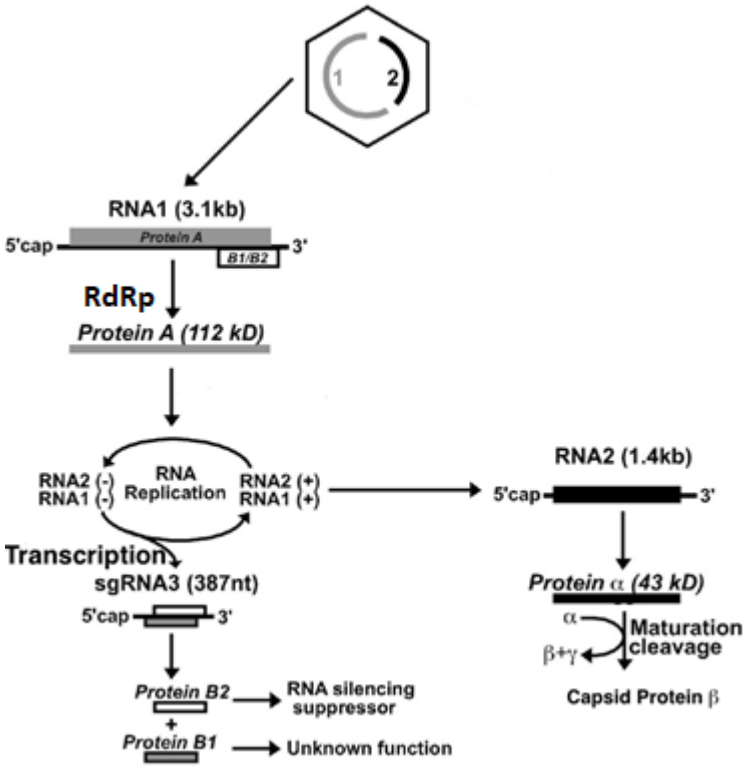

Figure 1: Protein synthesis in the lifecycle (see discussion in the text) of NoV[18].

CCMV is a positive-sense RNA plant virus with a multipartite genome encoding four genes contained in three single-stranded RNA (ssRNA) molecules. Like NoV, CCMV (whose

structure is shown in figure 2) is a spherical, icosahedral virus with a Caspar-Klug triangulation number of 3 (T=3 capsid)[Caspar and Klug 1962]. Figure 2 shows the icosahedral symmetry of CCMV, as determined by X-ray diffraction to a resolution of 3.2 Angstroms[Speir 1995]. demonstrates the capsid protein organization into this icosahedral symmetry. Our lab has demonstrated that the CCMV capsid protein can package any of a large variety of heterologous ssRNA *in vitro,* as long as the nt length does not significantly exceed that of the largest of the CCMV RNAs (3200nt). These *in vitro* assembled capsids are called virus-like-particles (VLPs), and have been shown to lend protection to the encapsidated RNA when the VLPs are incubated with RNases. Further, when CCMV VLPs containing fluorescent protein genes in mRNA or replicon form are transfected into mammalian cells, fluorescence is observed in the cells, confirming that the packaged cargo is being made available for translation within the cytosol[Azizgolshani 2013].

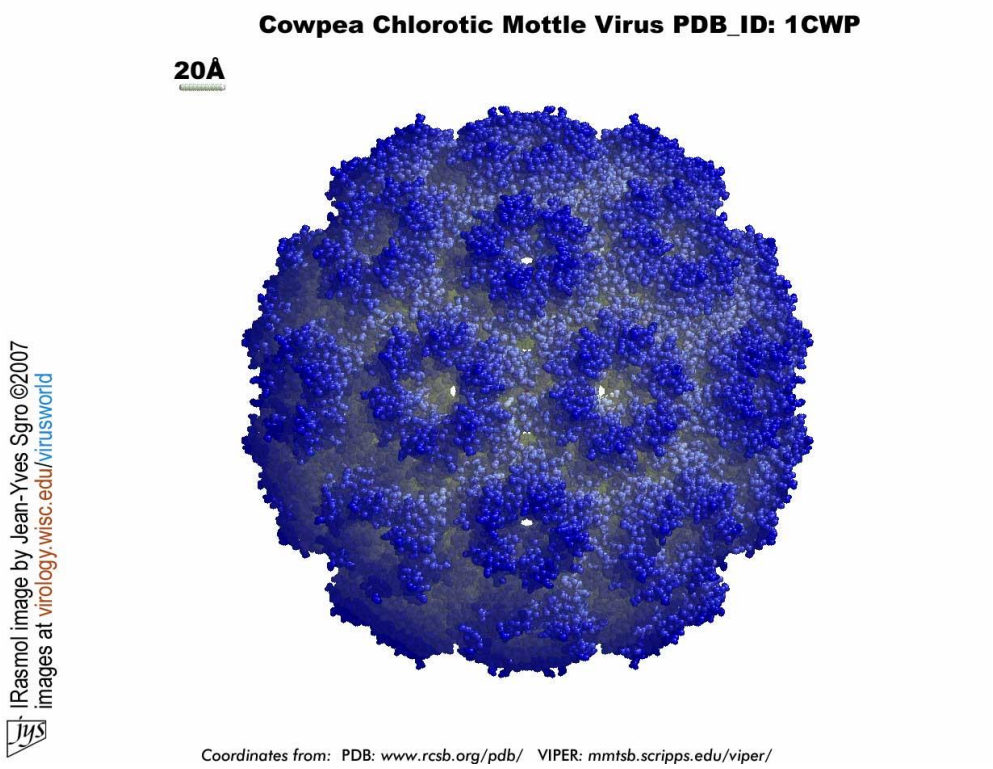

Figure 2: Structure of CCMV determined by X-ray Diffraction to a resolution of 3.2 Angstroms

To better characterize the uptake and amplification in mammalian cells of RdRp-coupled genes – both when naked or encapsidated – reporter genes such as enhanced yellow fluorescent protein (EYFP) or luciferase are used. A few modifications are required in order for RNA1 of NoV to be successfully transcribed and remain an active replicon while incorporating a gene of interest (GOI). Firstly, the plasmid construct for this replicon begins with a T7 promoter. At the start of RNA3, which makes up the subgenomic region, there is a premature stop codon introduced in the reading frame of the B2 RNA RNAi-silencing gene to provide the dual advantages of having expression of only the protein of interest (POI) from subgenomic replication while limiting the introduction of exogenous proteins. Since the GOI is both in the same reading frame and is initially translated along with the RdRp, a self-cleaving peptide

sequence (T2A peptide) derived from *Thosea asigna virus* is inserted immediately before the GOI. This replicon construct is described in more detail in Chapter 2, including a schematic in figure 3.

The first gene coupled to the replicon in this way was EYFP, a replicon provided by Dr. Leonid Gitlin of Dr. Raul Andino's group at UCSF. They also investigated the possibility of gene insertions into the subgenomic region of NoV[Gitlin 2014]. From transfections of baby hamster kidney (BHK) mammalian cells with this eYFP-replicon, we were able to follow the viral lifecycle by observing the emergence of fluorescence after 8 hours and following its gradual decrease after about 24 hours. In order to quantify the increased amount of protein expression due to amplification of these replicons, a luciferase replicon was also made. After transfection of equal copy numbers of either luciferase mRNA or luciferase-replicon mRNA, the luciferase activity was quantified using a luminometer at timepoints from 8 hours to 3 days. The luciferase-replicon generated at least 10 times the number of luciferase molecules as the luciferase mRNA over the course of the three days.

In collaboration with the German pharmaceutical company Boehringer Ingelheim (B-I), evaluation of possible efficacy of this platform for a cancer vaccine was begun by incorporation of a model antigen (Ovalbumin epitope) sequence into the replicon. Chapter 3 is a reformatted version of the published "Delivery of self-amplifying RNA vaccines in *in vitro* reconstituted virus-like particles"[Biddlecome 2019]. Because many immune cells are naturally primed to detect foreign virus particles and take them up by endocytosis, the targeting problem is already aided by the use of these VLPs. The sustained amplification of the antigen by the replicon will lead to increased translation of the model antigen, and this should allow for greater Ovalbumin antigen presentation by the major histocompatibility complex (MHC) of the immune cell.

Experiments involving incubation of EYFP-replicon VLPs with mouse or human dendritic cells – done in collaboration with the B-I corporate research labs in Ridgefield, Connecticut – have shown that VLPs are gaining entry into the dendritic cells. The dendritic cells incubated with VLP-packaged EYFP-replicon RNA exhibit greater expression of intracellular RNA and maturation markers than do the corresponding "naked" EYFP-replicon mRNA samples. Fluorescence activated cell sorting (FACS) allow for quantification of multiple surface antigens including our vaccine epitope or other antigens indicative of dendritic cell maturation.

Since most vaccines are administered incrementally in doses, an important factor is how the drug/vaccine is affected by existing immunity against the exposed, outer, portion of our VLPs. Antibodies were generated in Ridgefield against CCMV CP by immunizing mice with CCMV VLPs containing a non-translated RNA. These CCMV CP antibodies were pre-incubated with EYFP-replicon VLPs before incubating the VLPs with immature dendritic cells, leading to the observation of greater dendritic cell maturation compared to that of "naïve" VLPs, i.e., ones not exposed to antibodies. This work, as well as the mouse vaccination studies carried out by our B-I collaborators in Vienna, Austria, is described in Chapter 3. In particular, *in vivo* efficacy is demonstrated through a several-week serial immunization of mice by intravenous injection with the Ovalbumin-replicon VLP, Ovalbumin-replicon mRNA, or Ovalbumin protein, followed by assays of cytotoxic T-cell response, specifically the fraction of generated Ovalbumin-sensitive T cells.

Since RNA1 of NoV is already about the size of each genomic RNA packaged into CCMV, there is a limitation on the size of GOI that can be inserted. A promising avenue to allow for amplification of larger GOIs involves keeping RNA1 of NoV unchanged, and inserting the GOI into the also-replicated RNA2 of NoV which is also replicated. A previous study has shown

that by preserving the untranslated regions of RNA2 it is still replicated, even while substituting the capsid protein open reading frame with GFP. Co-transfection of wild-type RNA1 with RNA2 modified to include luciferase, showed that there is greater replication than both luciferase mRNA or the modified RNA2 alone. This work is described in Chapter 4.

While having a protected mRNA that can be self-amplified once it enters the cell is a promising therapeutic platform, the lack of specificity of delivery may be of concern for certain applications. For a vaccine aimed toward stimulation of cytotoxic cells by dendritic-cell MHC presentation of an antigen of interest, specific targeting may not be as crucial because dendritic cells are already primed to endocytose foreign particles. However, for many other applications that could benefit from a replicon-VLP strategy, such as delivery of a necessary protein that is compromised in diseased tissue, specific targeting of a cell type could be needed. Conjugation of an antibody to target the VLP to certain cell receptors can be used for this targeting. The most commonly used amino acids for this conjugation chemistry are lysine and cysteine. While CCMV has several surface-exposed lysines in each capsid protein, it was deemed useful to generate a cysteine-mutant CCMV so capsid protein subunits would have a single, unique thiol group available for maleimide or other chemistry. This work is described in Chapter 5.

Chapter 6 contains a short discussion of future directions, as well as a summary of conclusions.

Chapter 2: Nodamura replicon-containing molecule reporter gene expression and dilution effects

2.1 Nodamura RdRp-containing self-amplifying construct

To better characterize the uptake and amplification in mammalian cells of RdRp-associated genes – both when naked or encapsidated – reporter genes such as enhanced yellow fluorescent protein (EYFP) or luciferase are used. In order for RNA1 of NoV to be successfully transcribed and remain an active replicon (an RNA molecule that replicates itself) while incorporating a gene of interest (GOI), a few modifications are required. Firstly, the plasmid construct for this replicon (depicted in Figure 3, below) begins with a T7 promoter. In the beginning of RNA3, which makes up the subgenomic region, there is a premature stop codon introduced in the reading frame of the B2 RNA RNAi-silencing gene to provide the dual advantages of having expression only of the protein of interest (POI) from subgenomic replication while limiting the introduction of exogenous proteins. Since the GOI is both in the same reading frame and is initially translated along with the RdRp, a self-cleaving peptide sequence (T2A peptide) derived from *Thosea asigna virus* is inserted immediately before the GOI. The first gene coupled to the replicon in this way was EYFP. From transfections of baby hamster kidney (BHK) mammalian cells with this EYFP-replicon, we were able to follow the viral lifecycle by observing the emergence of fluorescence after 8 hours and following its gradual decrease after about 24 hours.

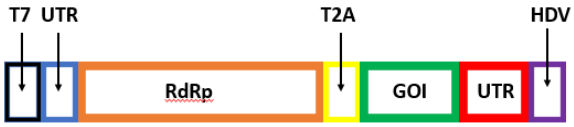

Figure 3: Schematic of the replicon construct used to amplify and express an arbitrary gene of interest (GOI). T7 is the transcriptional promoter, and the left and right UTRs are the 5' and 3' untranslated regions, respectively, of NoV RNA1 that are needed for replication. "RdRp" is the NoV RNA-dependent RNA polymerase. T2A is *Thosea asigna* virus 2A self-cleaving peptide that allows the RdRp-GOI polyprotein to function as two independent proteins, subsequent to translation. HDV is the Hepatitis Delta Virus ribozyme for ensuring clean RNA transcripts.

2.2 Quantitative and qualitative reporter gene studies of replicon expression

In order to quantify the increased amount of protein expression due to amplification of these replicons, a luciferase replicon was also made. After transfection by electroporation of equal copy numbers of either luciferase mRNA or luciferase-replicon mRNA into BHK cells, the luciferase activity was quantified using a luminometer at timepoints from 8 hours to 3 days, as shown in figure 4. The luciferase replicon generated at least 10 times the number of luciferase molecules as the luciferase mRNA over the course of the three days.

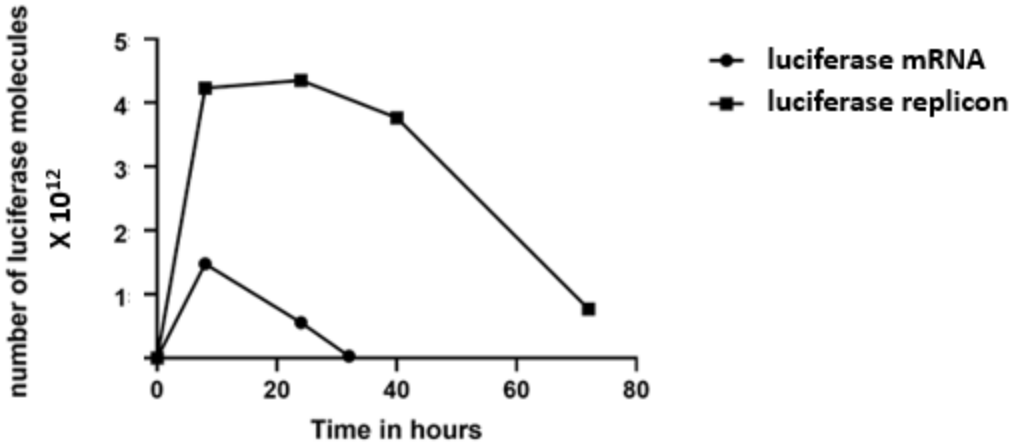

Figure 4: Time course of luciferase expression in BHK 21 cells. Electroporation of 10 million BHK cells with an equivalent copy number of replicon (5 µg), or luciferase mRNA (1.25 µg, less mass due to its shorter length). The plot shows the number of luciferase molecules as determined using the standard curves from the Promega renilla luciferase activity kit.

While the luciferase activity provides quantitative information about the increased protein expression from the replicon, it does not reveal qualitative information like the effect the replicon expression could have on cell morphology. To this aim we duplicated the transfection conditions, this time with eYFP in the replicon instead of renilla luciferase, and (as shown in figure 5), imaged the cells by fluorescence microscopy. After 17 hours there were many brightly fluorescent cells, and an approximately 75% transfection efficiency (the percentage of cells exhibiting fluorescence when comparing the brightfield image to the fluorescence image). When looking at this same plate of BHK cells after 41 hours, some interesting trends present themselves. For one, the percentage of cells exhibiting visible fluorescence decreases. Also, many of the fluorescent cells are round, indicative of dead or weak cells that are loosely attached. A fair number of detached cells were observed as early as 17 hours, some of which results from the harsh transfection method of electroporation. Still, the observations at 41 hours showing the

majority of fluorescent cells being detached from the plate suggests that an overabundance of replication can be damaging to the cell.

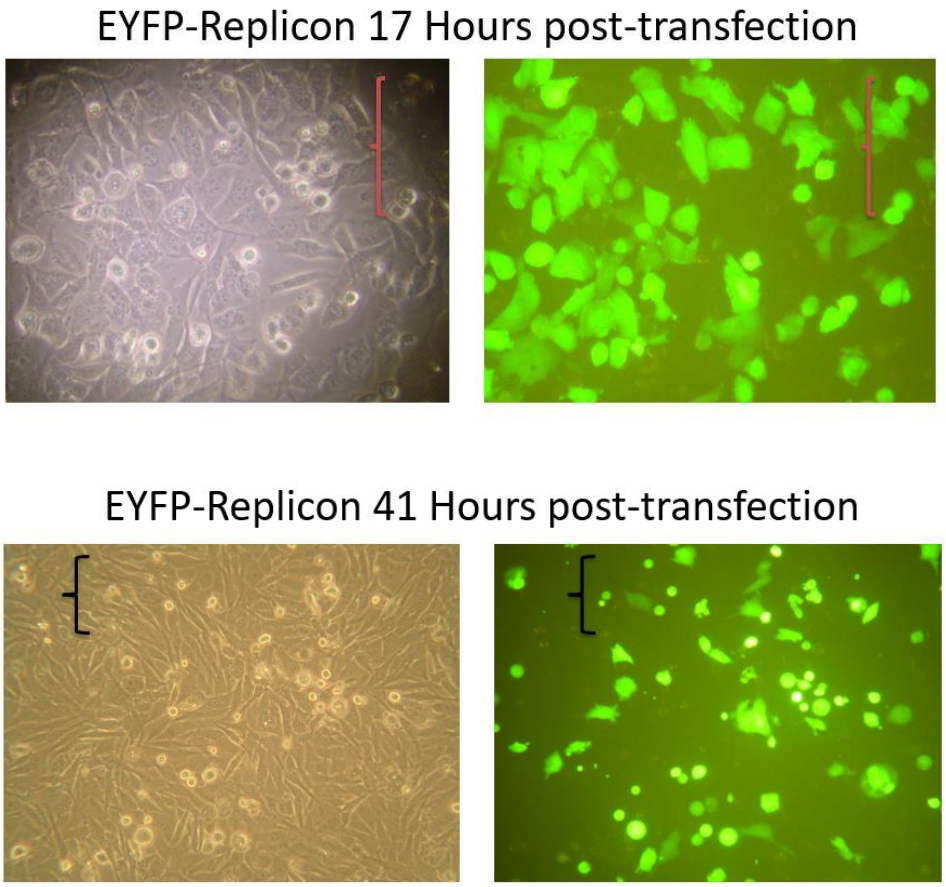

Figure 5: Fluorescence and brightfield microscope images of cells transfected with eYFP-Replicon after 17 and 41 hours.

2.3 Dilution experiments of replicon for effects on expression

While these studies utilize reporter genes in order to study the replicon, ultimately the aim is to use this replicon-VLP system as a therapeutic. One of the most expensive components of this platform is synthesizing capped RNA. The plasmid containing the replicon is transcribed

by a T7 promoter, and it is known that for each G nucleotide (up to 3 G's) at the end of this promoter sequence, the greater the yield of RNA from transcription. Since transcription using a T7 RNA polymerase begins with the first G nucleotide, the current replicon includes a single G at the beginning of the transcript. The RNA1 of *nodamura* naturally includes a G as its first nucleotide, so we wanted to investigate if adding the two extra Gs could increase transcriptional yield, and also to see if it has an effect on replication. As expected, the addition of the two extra Gs did increase the yield from transcription. When luciferase-replicon mRNAs with one and with three Gs are transfected in parallel into BHK cells, a 40% decrease in luciferase activity for the extra-Gs sample suggests that replication is being partially compromised. This attenuation from the extra Gs might be helpful to reduce the strain on cells that are becoming sick from host resources being diverted to support generation of exogenous proteins.

Another method explored for attenuating the replicon activity, was to deliver less to each cell. While a transfection experiment involves a great excess delivered to each cell, for in vivo applications a much smaller number of molecules make it into each cell. We performed transfections at varying numbers of luciferase mRNA and replicon in order to understand the dose dependence for each. Lipofectamine forms cationic liposomes around RNA. The cationic liposomes work to permeabilize cell membranes to allow entry of nucleic acid. It is important in these experiments to maintain the same number of lipoplexes so each cell encounters at least one lipoplex even at low copy number of transfected mRNA; accordingly, the total mass of RNA for each transfection is maintained by addition of uncapped – and therefore untranslatable – RNA of similar length (pTRI-XEF for luciferase mRNA, and pB1/B3 for luciferase replicon).

While for luciferase mRNA we observed a roughly linear dependence of activity with increasing mass of mRNA transfected, the dose dependence for the replicon is markedly

different. A time course for high concentrations of separately transfected luciferase mRNA and replicon reveal similar profiles of luciferase activity – see figure 6. The maximum number of luciferase molecules reach similar peaks, and the decline over time is only moderately extended for the luciferase replicon samples, but at later time points the replicon cell samples show more signs of sickness/death than the samples treated with luciferase mRNA.

At low concentrations of mRNA, the luciferase activity for the mRNA samples is very low. In contrast, the activity for the replicon is only slightly decreased compared to the transfection that involves 40 times the mass of replicon mRNA – see Figure 7. In fact, we find that luciferase activity plateaus at higher concentrations of transfected replicon. We see similar or even greater numbers of luciferase molecule as the number of replicon molecules transfected is decreased. Additionally, we see an extended period of time during which there is significant replication for lower concentrations of replicon.

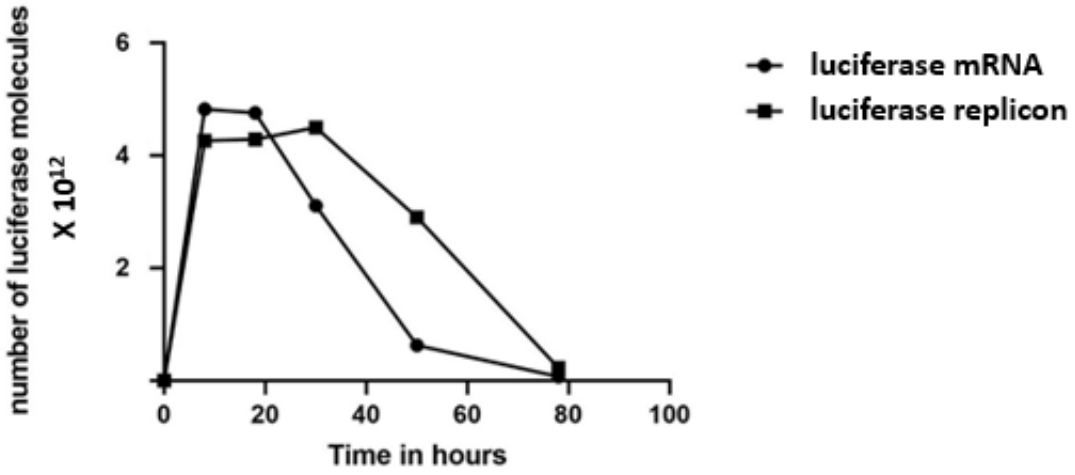

Figure 6: Time course of luciferase expression in BHK 21 cells with higher concentration transfection. Cells were transfected using lipofectamine with either 500 ng of replicon or 125 ng of luciferase mRNA.

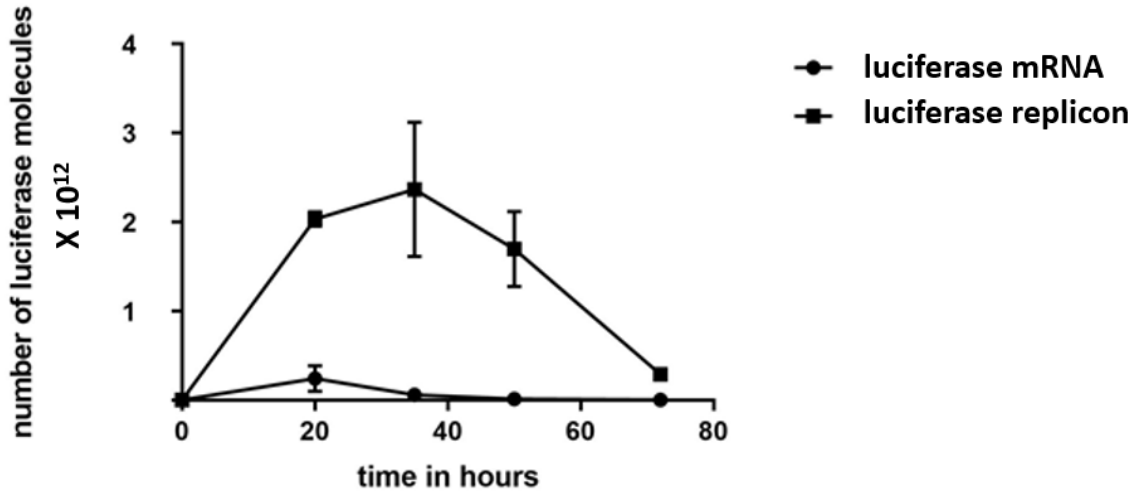

Figure 7: Time course of luciferase expression in BHK 21 cells with lower concentration transfection. Cells were transfected using lipofectamine with either 12.5 ng of replicon or 3 ng of luciferase mRNA.

These dilution experiments showed that low numbers of replicon can still result in significant levels of protein expression of any gene of interest. At low numbers of replicon making into a cell, as would be the probable scenario for an *in vivo* application, we could have an amplification of protein yield without the detrimental effects of too much replication, as seen in figure 5.

2.4 Materials and Methods

Cloning of Replicon Constructs

Refer to section 3.5, *Cloning of Replicon Constructs*

In Vitro transcription of replicon, reporter mRNA, and carrier RNA

The plasmids were linearized with XbaI and subsequently purified using QIAquick PCR purification columns from Qiagen (Valencia, CA, USA). The linearized DNA was transcribed with T7 RNA polymerase. The buffer composition of the reaction was 40 mM Tris pH 7.5, 25 mM $MgCl_2$, 4 mM µl DTT, and 2 mM spermidine. The rNTP concentration was 7.5 mM. Incubation was for 3 hours at 37°C, followed by a 30-minute incubation with turbo DNase at the same temperature. The resulting RNA was purified using the RNeasy mini kit from Qiagen, and replicon and reporter gene RNA was then capped using the Vaccinia Capping System from New England Biolabs (Beverly, MA, USA). This process added a 7-methylguanylate cap structure to the 5' end of RNA in the presence of the capping enzyme, reaction buffer, GTP, and the methyl donor, SAM. The *in vitro* transcription and capping were both done in the presence of RNase inhibitors to preserve the RNA, and the capping mixture was again purified by an RNeasy mini column (Qiagen).

Electroporation of BHK 21 cells

In preparation for electroporation, cells were passaged the day before until they were at about 70-90 percent confluence. The cells were washed with chilled and RNase-free PBS, after aspirating the media. Trypsin-EDTA (0.25%) was added to detach cells, then after cell detachment, media was added back to standard capacity (10 ml for 10-cm, and 25 ml for 25-cm plates). The cell mixture was dispensed into tubes, and centrifuged at 500xg for 3 minutes at room temperature. After aspiration, pellets were washed in more PBS and trypsin added up to half initial the amount. This washing step was repeated, again halving the amount of trypsin.

Cells were counted using a hemocytometer. 10 µl of the 50-ml cell suspension was pipetted between the hemocytometer and the cover slide. Using a cell counter, the number of cells in each

larger grid was taken(4-5 bigger square grids for greater accuracy). The relation for determining total cells in suspension was the following:

$$\frac{\#\ total\ cells}{\#\ bigger\ square} \times 10^4\ \frac{cells}{ml} \times 50\ ml = \#\ cells\ in\ suspension$$

Electroporation with the known number of washed, healthy cells involved spinning the cells down and resuspending them in a volume that gave a concentration of 20 million cells/ml. 500 µl of cells were mixed with 5 µg mRNA and then dispensed into a cuvette. The gene pulse was set to high range, high capacitance to 25, voltage to 15 volts. After pulsing twice, cells were replated onto a 10-cm cell culture plate. The cuvette was washed with 500 µl buffer to recover the remaining cells.

Lipofectamine Transfection, including RNA dilutions, of BHK 21 cells

Refer to section 3.5, *BHK Cell Culturing and Transfections*

Luciferase Assay

Refer to section 3.5, *Luciferase Assay*

Chapter 3: Self-amplifying RNA vaccines in *in vitro* reconstituted virus-like particles

Abstract

Many mRNA-based vaccines have been investigated for their specific potential to activate dendritic cells (DCs), the highly-specialized antigen-presenting cells of the immune system that play a key role in inducing effective $CD4^+$ and $CD8^+$ T-cell responses. In this chapter we report a new vaccine/gene delivery platform that demonstrates the benefits of using a self-amplifying ("replicon") mRNA that is protected in a viral-protein capsid. Purified capsid protein from the plant virus *Cowpea Chlorotic Mottle Virus* (CCMV) is used to *in vitro* assemble monodisperse virus-like particles (VLPs) containing reporter proteins (e.g, Luciferase or eYFP) or the tandem-repeat model antigen SIINFEKL in RNA gene form, coupled to the RNA-dependent RNA polymerase from the *Nodamura* insect virus. Incubation of immature DCs with these VLPs results in increased activation of maturation markers – CD80, CD86 and MHC-II – and enhanced RNA replication levels, relative to incubation with unpackaged replicon mRNA. Higher RNA uptake/replication and enhanced DC activation were detected in a dose-dependent manner when the CCMV-VLPs were pre-incubated with anti-CCMV antibodies. In all experiments the expression of maturation markers correlates with the RNA levels of the DCs. Overall, these studies demonstrate that: VLP protection enhances mRNA uptake by DCs; coupling replicons to the gene of interest increases RNA and protein levels in the cell; and the presence of anti-VLP antibodies enhances mRNA levels and activation of DCs *in vitro*. Finally,

preliminary in vivo experiments involving mouse vaccinations with SIINFEKL-replicon VLPs indicate a small but significant increase in antigen-specific T cells that are doubly positive for IFN and TFN induction.

Keywords: self-replicating RNA, *in vitro* self-assembly, virus-like particles, dendritic cell activation, successive-vaccination boosts

3.1 Introduction to a replicon-based mRNA VLP delivery platform as a vaccine

The delivery of RNA genes has great potential in a range of therapeutic applications[Lam 017, Geall 2012, Brito 2014, Chahal 2016, Rohovie 2017], with the advantage – compared to DNA gene delivery – that there is no nuclear localization and thus no possibility of genomic integration. Some disadvantages it poses for gene delivery include its vulnerability to ribonuclease (RNase) digestion and – in the case of non-vaccine genes – its triggering of innate immune responses[Shoggins 2011, Schott 2010]. Another limitation for *in vivo* applications is that gene expression in targeted cells does not have any amplification, resulting in transient and low expression levels. Accordingly, a gene delivery platform that includes *self-amplifying* mRNA inside a *protective* capsid allowing for cell targeting and uptake[Destito 2007, Hovlid 2012, Kovacs 2007, Stephanopoulos 2010] could represent a major step forward in mRNA-based gene therapy. We address these issues by using viral replicons (self-replicating RNA molecules) for the self-amplification, and *in vitro* self-assembled virus-like particles (VLPs) for the

protection, specifically using the RNA-dependent RNA polymerase (RdRp) from *Nodamura virus* (NoV) and capsid protein from *Cowpea Chlorotic Mottle virus* (CCMV).

NoV is a positive-sense RNA insect virus with a bipartite genome whose two molecules are co-packaged in the same virion[Johnson 2003]. The larger RNA molecule includes the RNA1 [≈ 3200 nucleotides (nt)] gene that encodes for the RdRp, and a subgenomic RNA3 (≈ 400 nt) encoding the B2 protein that suppresses host-cell RNA interference[Sullivan 2005]. The other molecule is the (≈ 1350 nt) RNA2 that encodes the capsid protein. In addition to replicating in natural insect hosts such as Drosophila, NoV has been shown to also have strong RdRp-dependent replication in mammalian cells[Johnson 2004]. Further, it has been demonstrated that – not only its own genes - but also any gene of interest can be amplified if inserted into the subgenomic region of RNA1 directly after the RdRp open reading frame and before the 3' untranslated region (UTR)[Gitlin 2014].

CCMV is a positive-sense RNA plant virus with a tripartite genome of four genes contained in three single-stranded RNA (ssRNA) molecules[Speir 1995]. Like NoV, CCMV is a spherical, icosahedral virus whose capsid has a Caspar-Klug triangulation number of 3[Caspar 1962]: each of the CCMV ssRNAs is separately packaged in a T=3 shell of 180 subunits, organized as 12 pentamers and 20 hexamers of a single capsid protein[Speir 1995]. It has been demonstrated that the CCMV capsid protein can package any of a large variety of heterologous ssRNA *in vitro* into wildtype capsids, as long as the length lies in the range 2500-4200nt so that it does not significantly differ from that (3200nt) of the largest of the CCMV RNAs[Cadena-Nava 2012, Garmann 2014a, Garmann 2014b, Garmann 2016]. These *in vitro* assembled capsids, known as virus-like particles (VLPs) – and in particular ones containing RNA replicons – have been shown[Azizgolshani 2013] to both lend protection to the encapsulated RNA when

incubated with RNases, and make available its genetic cargo to translation upon delivery to mammalian cells. Because of the unique ability of CCMV capsid protein to package heterologous RNA into perfectly-monodisperse icosahedrally-symmetric (26-nm/180-protein) nanoparticles[Cadena-Nava 2012, Garmann 2014a, Garmann 2014b, Garmann 2016], the virus-like particles we use as self-replicating gene-delivery vectors are uniquely well-characterized. Similar results have been demonstrated with cylindrical VLPs reconstituted with capsid protein from *Tobacco Mosaic Virus* (TMV) and RNA replicons from *Semliki Forest Virus*, with the replicons requiring that a TMV "origin-of-assembly"/packaging sequence be inserted into them[Kemnade 2014].

It is a feature of our replicon gene delivery platform that the gene of interest is coupled to the replication and translation of the NoV viral components, so that it has the capability of being used for a large array of possible therapies. Here we use the reporter proteins luciferase and enhanced yellow fluorescent protein (eYFP) to characterize and quantify the coupling of RNA replication and protein expression by the replicon. We then evaluate the efficacy of this platform for delivering antigens in RNA form by incorporating into the replicon a model antigen sequence (Ovalbumin epitope SIINFEKL[Carbone 1992]). Since many immune cells are naturally primed to detect foreign virus particles and take them up by endocytosis, the targeting problem is already partially solved for these VLPs. The sustained amplification of the antigen sequence by the replicon leads to increased translation of the model antigen, and this allows for greater marker activation and Ovalbumin antigen presentation by the major histocompatibility complex I (MHC I) of the immune cell – see Figure 8.

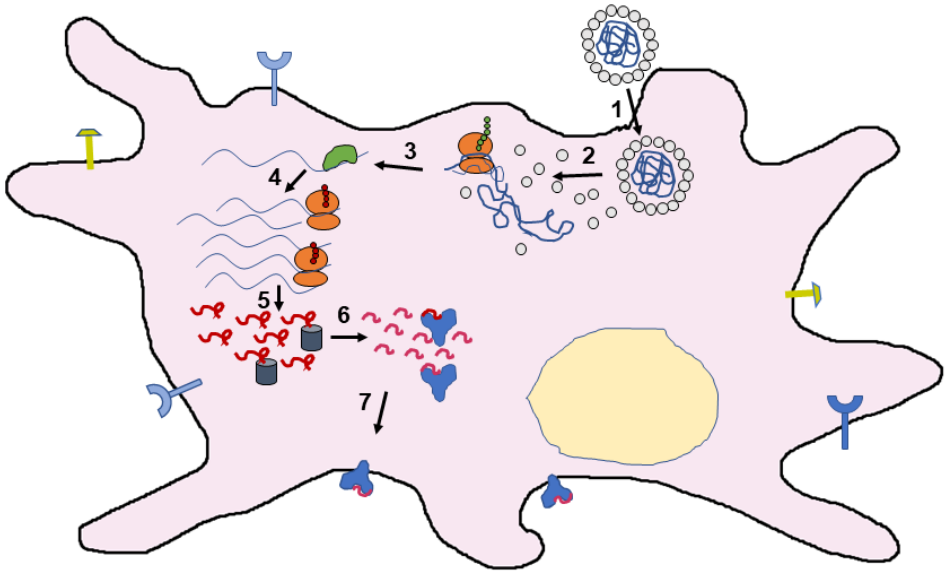

Figure 8. Schematic of DC activation triggered by VLP delivery of a self-replicating vaccine. Upon uptake (1), disassembly (2) of the VLP makes its RNA gene content accessible to the ribosomal machinery (red small and large subunits). Of the two protein gene products – the RdRp of the Nodamura virus, and the tandem OVA SIINFEKL epitope repeats – only the RdRp (green blob) is shown (3). There follow (4) many rounds of replicon amplification (by the RdRp) and translation of OVA repeats (long red squiggles), and subsequent processing (5) of the repeats by proteasomes (grey cylinders) and charging (6) of MHC-I molecules (blue Ys) with individual SIINFEKL epitopes (short red squiggles), which are then secreted (7) for presentation at the plasma membrane, along with CD 80, 86, and MHC-II molecules (lollipops).

In this paper we demonstrate that amplification of reporter genes by the NoV replicase results in much greater protein expression than an equal copy number of the reporter gene mRNA alone. Further, when immature DCs are incubated with VLPs containing this replicon mRNA significant increases in DC maturation and RNA levels of the gene of interest (eYFP or the tandem OVA SIINFEKL epitope) are observed. The samples with *un*packaged mRNA or replicon mRNA show no perceptible change in maturation or RNA levels compared to negative controls, pointing up the fact that the VLP effectively protects the mRNA and helps it gain entry into the DCs.

Because many vaccines need to be administered incrementally in doses, an additional important factor is how the drug/vaccine is affected by existing immunity against the exposed outer portion of VLPs. Accordingly, antibodies were generated against CCMV capsid protein (CP) by immunizing mice with CCMV VLPs containing a non-translatable RNA. VLPs containing eYFP-replicon or OVA-replicon were incubated with these polyclonal anti-CCMV CP antibodies before being added to immature DCs, leading to enhanced DC maturation and RNA levels of eYFP or OVA compared to those of "naïve" VLPs, i.e., ones that have not been exposed to antibodies.

Finally, in preliminary in vivo experiments, we have measured the T-cell response to a series of mouse vaccinations with VLPs containing the SIINFEKL antigen in replicon form, and find a small but significant population of SIINFEKL-sensitive T cells that are doubly-positive in INF and TFN cytokine production.

Hijacking of the Nodamura virus life cycle

Figure 9A, which is adapted from Ball, et al.[25] shows the protein synthesis components of the NoV life cycle, depicting schematically the replication and translation strategies of this two-molecule/four-gene positive-sense RNA virus. Molecule RNA1 is translated directly to yield "Protein A", the RdRp that binds RNA1 and RNA2 and replicates them strongly through successive rounds of -strand and +strand synthesis. As part of the replication of RNA1 its -strands are "transcribed" to give not only +strands of the full-length RNA1, but also mRNA (subgenomic [sg] RNA3) that is translated to either a B1 protein in the same reading frame as the RdRp, or a B2 protein in an alternate reading frame. The B2 protein is known to suppress host-cell RNA interference[Johnson 2004], whereas the function of B1 has not yet been determined. RNA2 is translated to capsid protein alpha, which assembles into a capsid in which the protein matures by undergoing autocatalytic cleavage to yield capsid protein beta and the membrane-permeabilizing peptide gamma.

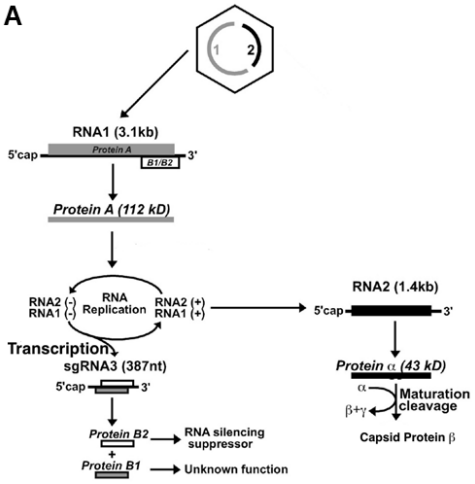

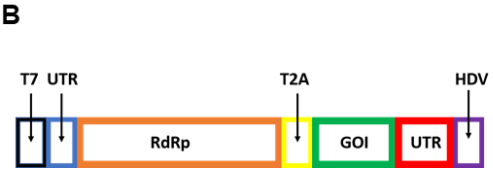

C

Gene of Interest	Purpose
Fluorescent Protein eYFP	Visualization of replicon lifecycle
Renilla Luciferase	Quantification of protein expression
Ovalbumin tandem epitope SIINFEKL	Maturation of dendritic cells and antigen presentation

Figure 9. **A Protein synthesis in the lifecycle (see discussion in the text) of NoV**[18]. **B Schematic of the replicon construct used to amplify and express an arbitrary gene of interest (GOI)**. T7 is the transcriptional promoter, and the left and right UTRs are the 5' and 3' untranslated regions, respectively, of NoV RNA1 that are needed for replication. "RdRp" is the NoV RNA-dependent RNA polymerase. T2A is *Thosea asigna* virus 2A self-cleaving peptide that allows the RdRp-GOI polyprotein to function as two independent proteins, subsequent to translation. HDV is the Hepatitis Delta Virus ribozyme for ensuring clean RNA transcripts. **C** Table of genes of interest, inserted one at a time into the replicon depicted in B.

3.2 Generation and characterization of ovalbumin epitope-containing replicon VLPs

In the present work we dispense with RNA2 and add a gene of interest (GOI) to the subgenomic sequence of RNA (see METHODS), as shown in Figure 9B. Any gene of interest can be coupled to the replication of the RdRp by inserting it in this way, but its length must be less than about 1000 nt in order to guarantee *in vitro* packaging[Cadena-Nava 2012, Garmann 2014a, Garmann 2014b, Garmann 2016] of the ensuing replicon by CCMV CP into a single RNase-resistant wildtype (T=3) capsid. This GOI-containing replicon is constructed in a plasmid that can be transcribed *in vitro*, and includes other important features such as a self-cleaving peptide sequence (T2A peptide) derived from *Thosea asigna virus*, which separates the viral and exogenous proteins to render them functional, and a Hepatitis-Delta-Virus (HDV) ribozyme for providing monodisperse RNA transcripts.

Depending on the goal of our assay, we use one of several GOIs (see table in Figure 9C): eYFP for direct qualitative visualization of replicon replication and translation; Renilla Luciferase for quantification of the resulting level of protein expression from the replicon; and tandem repeats of the SIINFEKL epitope of Ovalbumin for quantification of DC maturation (marker protein expression) and antigen presentation, and for future follow-up *in vivo* experiments assaying T-cell response in mice.

Reporter genes in replicon form are strongly replicated and expressed

Figure 10A shows the time courses for luciferase protein yield from baby hamster kidney (BHK) cells transfected by lipofectamine with replicon versus naked mRNA forms of luciferase, emphasizing the 30-fold greater yield found for the replicon, and its persistence over several days. Along with the 30-fold greater yield of luciferase molecules, a 150-fold increase in RNA molecules including the luciferase gene is observed with the replicon (figure 10B).

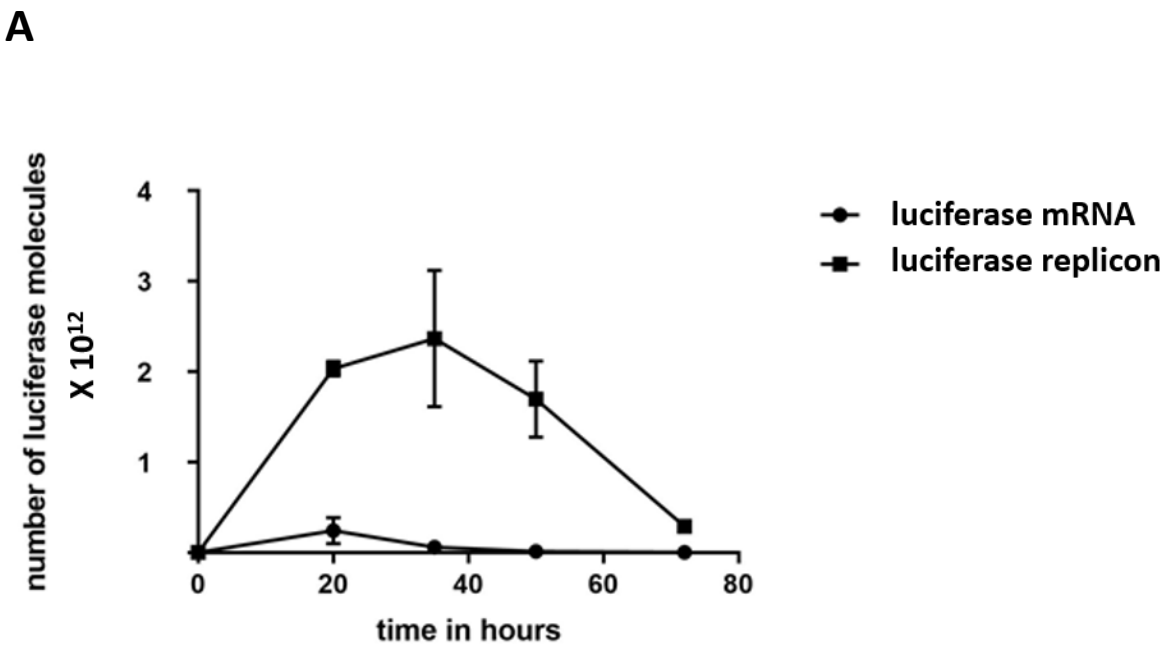

B

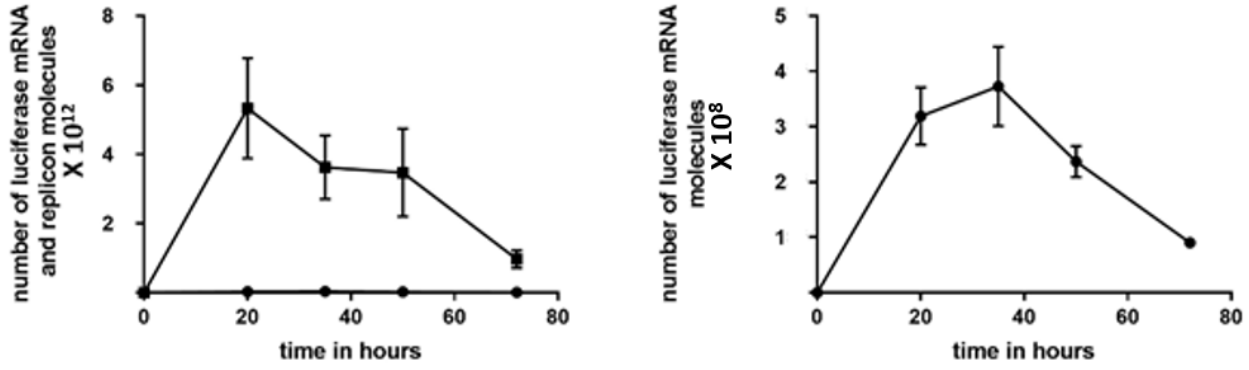

Figure 10. A Time course of luciferase expression in BHK-21 cells. Cells were transfected with equal numbers of renilla luciferase gene, in mRNA form ("luciferase [luc] mRNA") – including a poly-A tail – or as NoV replicon with luciferase in the sub-genomic region ("luciferase replicon [luc-rep] RNA"). The plot shows the estimated number of luciferase molecules as determined using the standard curves from the Promega renilla luciferase activity kit. **B Number of luc mRNA (solid circles) and luc-rep RNA (solid squares) molecules at each of the time points in A**. These numbers were determined by real-time quantitative PCR (qPCR), with results for both luciferase activity and qPCR from biological duplicates. Each of those biological duplicates was measured in duplicate or triplicate for luciferase activity and qPCR, respectively. Of these replicates, the average is plotted with standard deviation (in some cases the error bar is narrower than the data point itself, thus is not included). The figure on the right is a re-plotting – with an expanded scale in the units of 10^8 instead of 10^{10} – of the mRNA numbers that are indistinguishable from zero in the figure on the left.

Nodamura replicons can be *in vitro* packaged into and protected by virus-like particles

Figures 11A and 11B show gel and electron micrograph images and size histograms, respectively, of *in vitro* reconstituted VLPs prepared (see METHODS) from purified CCMV CP and *in vitro* transcribed eYFP replicon RNA. All figures are for samples that have been treated with RNase, confirming that the VLPs are able to protect RNA cargo. Note that the reconstituted VLPs run a little slower than the wildtype virions because they are prepared from a small excess of protein (see discussion in Materials and Methods) that binds to the outside of the self-assembled capsid.

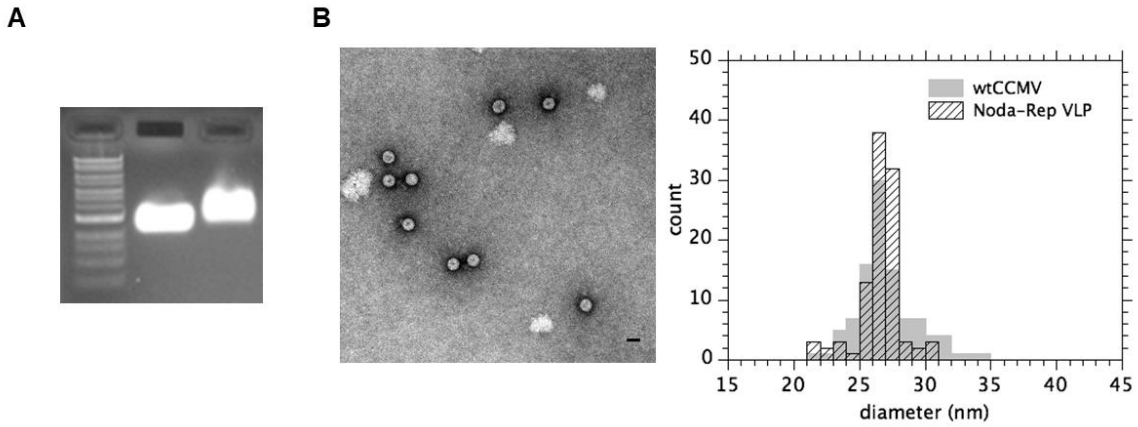

Figure 11. Verification of replicon VLP assemblies. **A)** A native 1% agarose gel with (left to right) a NEB 1 kb DNA ladder, wild-type CCMV virion, and reconstituted VLPs containing NoV replicon RNA.**B) LEFT.** Negative-stain electron microscopy (EM) image of *in vitro* self-assembled VLPs containing eYFP replicon mRNA. **B) RIGHT**. Histogram of size distribution of

VLPs shown in the electron micrograph, juxtaposed on the corresponding histogram of sizes for wildtype CCMV virions.

3.3 RNA quantitation and maturation markers showing activation of immature dendritic cells when incubated with replicon-VLPs

DCs maturation and RNA replication are strongest for packaged replicons

Figure 12Ai shows panels of CD86, MHCII and CD80 marker activation, determined by flow cytometry, following incubation of immature DCs with medium, naked eYFP mRNA, CCMV VLPs carrying eYFP mRNA, naked eYFP replicon mRNA, and CCMV VLPs carrying eYFP replicon mRNA. Fig. 5Aii shows the RNA levels corresponding to each of these five incubations, determined by qPCR, and plotted as numbers relative to those of the housekeeping gene beta-actin. Consistent with the well-known fact that DC maturation is extremely sensitive to culturing conditions, e.g., to medium and pipetting, marker activation by media is comparable to that by our "active" reagents, except for the case of replicon-containing VLPs. RNA replication – see Fig. 5Aii – is present only for the replicon reagents and is 100 times greater for the packaged replicon. The sensitivity of DC maturation to donor cells is seen in Figure 12B, where DCs from a different donor than in 5A are used for incubations with medium (negative control), naked eYFP replicon mRNA, and CCMV VLPs carrying eYFP replicon mRNA. Here, while there is again comparable maturation associated with medium as with the naked replicon, the activation is one to two orders-of-magnitude greater for the VLP-packaged replicon.

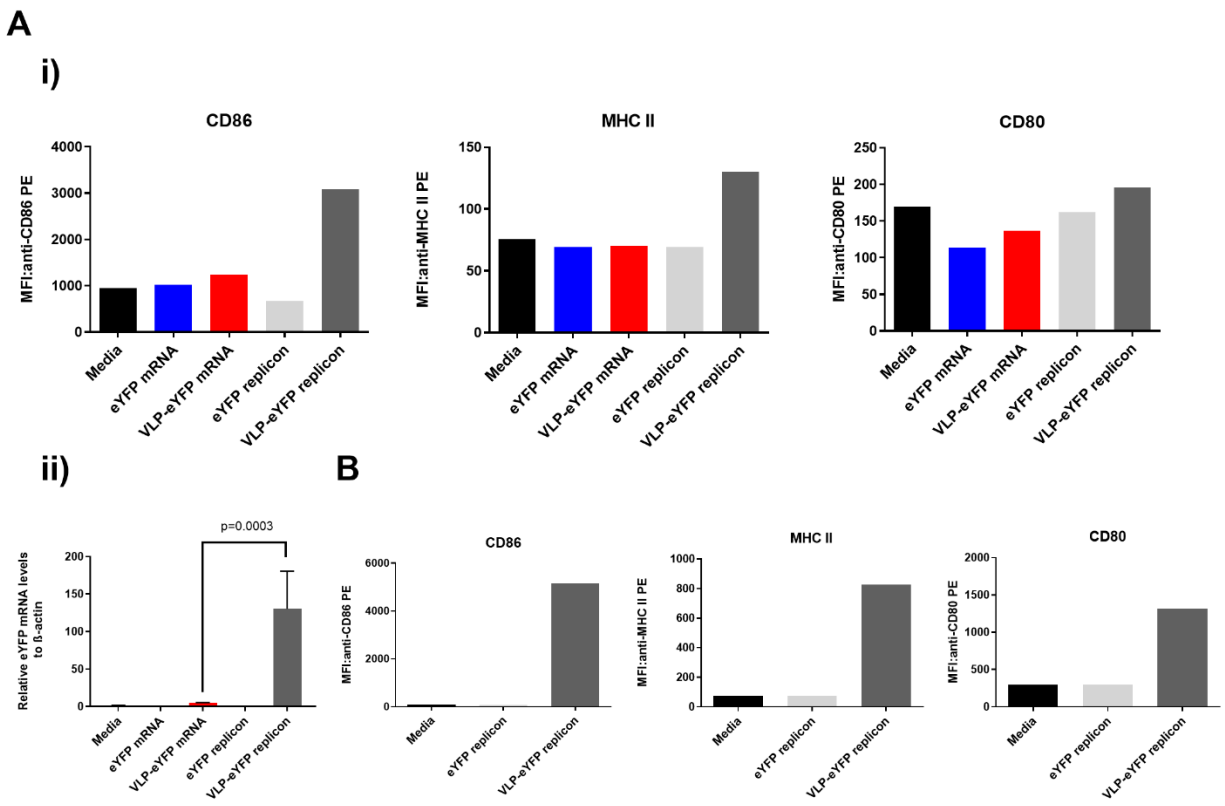

Figure 12. Expression intensity of activation markers on DCs. **A i)** Results from a donor treated with different conditions of EYFP mRNA or CCMV VLPs. The median fluorescence intensity (MFI) of CD86 (left), MHC II (middle) and CD80 (right) was determined by FACS assays for cells treated with media only (black bars), eYFP mRNA (blue bars), CCMV VLPs carrying eYFP mRNA (red bars), eYFP replicon mRNA (light grey bars), or CCMV VLPs carrying eYFP replicon (dark grey bars). **A ii)** RNA quantitative PCR (qPCR). The same-donor DCs treated/incubated with each of the five reagents in Ai were lysed after 24 hours and eYFP-specific mRNA levels were determined by qPCR. Their numbers relative to beta-actin multiplied by 1000 are plotted. From the same sample of dendritic cells assayed for maturation markers, triplicate measurements yielded the plotted average and standard deviation (p value was determined using a one-way Anova test). **B** Maturation markers probed as in Ai but with DCs

from a different donor, for incubations with media only (black bars), eYFP replicon mRNA (light grey bars), and CCMV VLPs carrying eYFP replicon mRNA (dark grey bars).

Pre-incubation of VLPs with VLP-antibodies enhances DC activation and RNA replication

To check whether antibodies against the CCMV VLPs can modulate the RNA uptake and activation of DCs, mice were immunized three times subcutaneously (see METHODS) with CCMV VLPs containing a non-translated RNA. Pre- and post-immune sera were collected and antibody titers were determined by ELISA against the CCMV VLPs. As shown in Figure S1, strong antibody responses were observed in all of the animals.

Figure 13 shows (top) the enhancement of DC marker activation when DCs are incubated with VLPs that have been exposed to capsid protein antibodies (in the form of serum from CCMV-inoculated mice). Here the packaged replicon includes the OVA tandem repeats, rather than eYFP. Again the enhanced marker activation associated with the pre-incubated VLPs correlates with a much larger enhancement in the level of RNA replication (see Figure 13 BOTTOM).

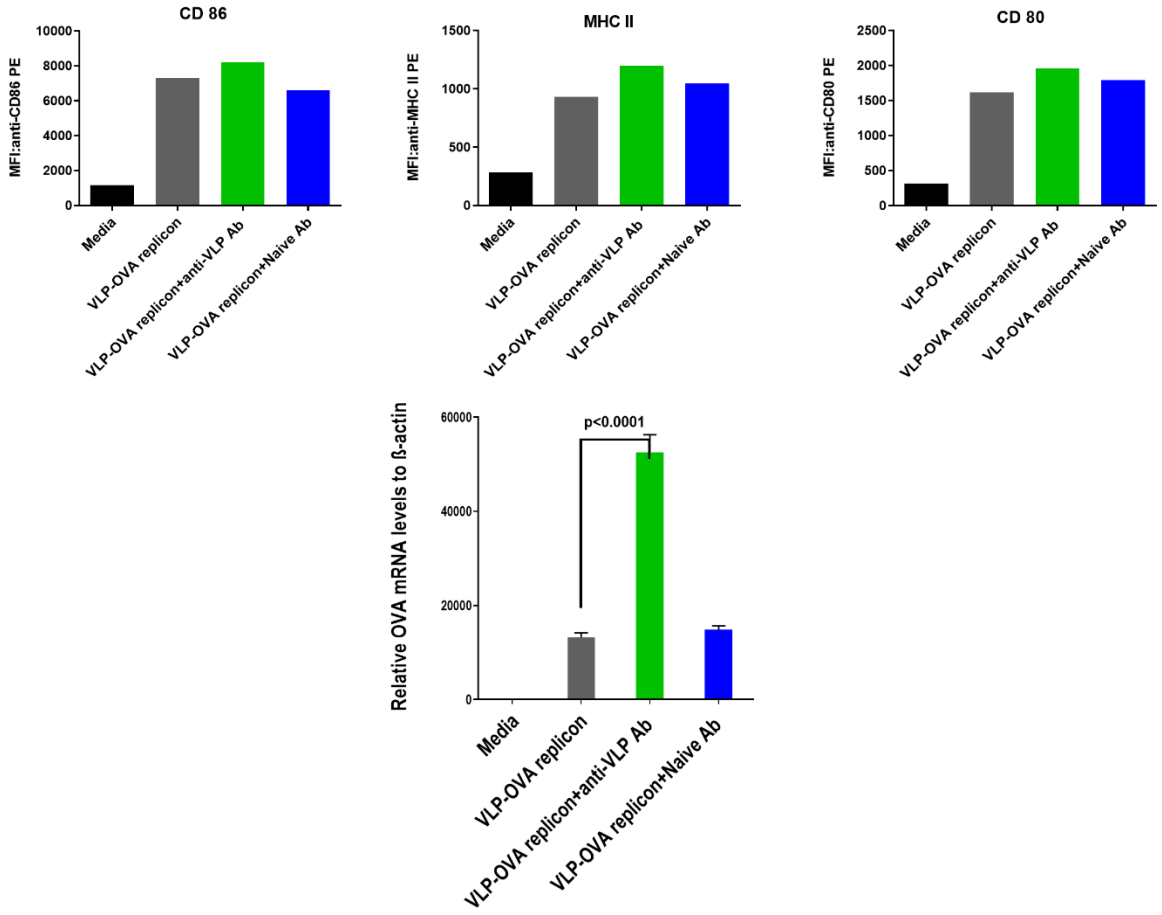

Figure 13. TOP: Expression intensity of activation markers on DCs treated with pre-incubated OVA-Replicon VLPs. The median fluorescence intensities (MFIs) of CD86 (left), MHC II (middle) and CD80 (right) were determined for cells treated with media only (black bars), CCMV VLPs carrying OVA replicon mRNA (grey bars), or CCMV VLPs carrying OVA replicon that have been pre-incubated with anti-CCMV VLP (green bars) or naïve serum antibodies (blue bars).

BOTTOM: RNA qPCR. DCs treated with one or another of these three "reagents" were lysed and Ova-specific mRNA levels were determined by qPCR (again measured in triplicate as in Figure 12 Aii). The p value was determined using a one-way Anova test.

Similar results are obtained with the same donor cells for VLPs containing the eYFP replicon – see Figure S2 – i.e., marker activation is enhanced by pre-incubation with anti-CCMV VLP antibody, again associated with a much greater enhancement of RNA replication.

3.4 Mouse vaccination with ovalbumin-replicon VLPs induces specific T-cell response

In a preliminary *in vivo* study we vaccinated mice with in vitro reconstituted CCMV VLPs containing the SIINFEKL replicon RNA. Three subcutaneous (s.c.) injections consisting of 100µg of VLP in a 100µl volume were administered, separated by an interval of one week, and on the 4^{th} week ex vivo analyses of spleen T cells were carried out by FACS. The negative control experiment ("Ctr") was a corresponding series of injections of buffer solution, and the positive control was the T-cell analysis of a 96:4 mixture of T-cells from wildtype mice and from OT-1 mice engineered with a SIINFEKEL-specific T-cell receptor. As seen in Figure 14 there is a small (0.4%) but significant T-cell response to the SIINFEKL replicon VLPs. Similarly, there is a small but significant increase in the percentage of T cells that are doubly positive for induction of both IFN γ and TNFα; see Figure S3.

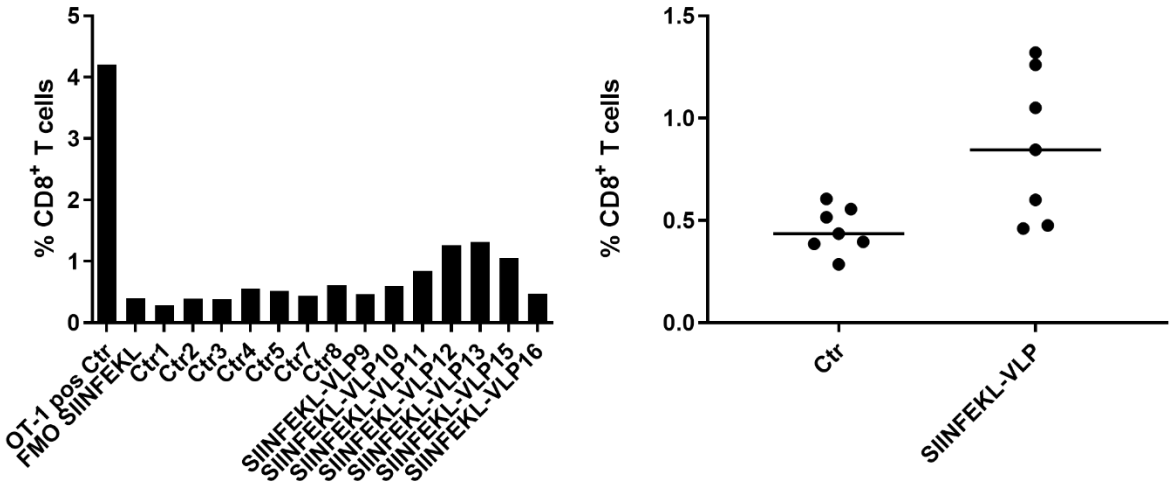

Figure 14. Percentage of SIINFEKL specific CD8$^+$ T-cells from mice vaccinated three times, separated by one-week intervals. Cells isolated from spleens were analyzed ex vivo by flow cytometry one week after the last vaccination.

LEFT: The positive control ("OT-1 pos Ctr", left-most bar) is the result from a 4:96 mixture of splenocytes from an OT-1 mouse (homozygous for the transgenic T cell receptor recognizing SIINFEKL in the context of H-2Kb) and from a wildtype mouse; it provides a calibration of SIINFEKL-specific T-cell percentages harvested from the vaccinated mice. "FMO (fluorescence minus one) SIINFEKL" refers to a negative control in which the H-2Kb/SIINFEKL Pentamer is absent from the fluorochrome mix used for flow analysis. The "Ctr" measurements involve 7 wildtype mice (1-5, 7&8) vaccinated with buffer solution, while the"SIINFEKL-VLP" data refer to mice (9-13, 15-16) vaccinated with buffer with SIINFEKL replicon VLPs.

RIGHT: The same data are presented as scatter plots, including the median (line) for each set of measurements. An unpaired t-test with Welch's correction was performed and a significant difference between the groups was seen (p=0.0248).

3.5 Conclusions

We have shown that levels of DC activation are significantly enhanced by incorporation of reporter genes and model antigens into self-replicating RNA molecules – replicons – that have been *in vitro* packaged into VLPs. This enhancement of marker protein expression has been correlated with a much stronger amplification of RNA replication of the replicons, corresponding to RNA levels as much as ten-thousand-fold greater than those of the housekeeping protein beta-actin. Further enhancement of DC activation and RNA replication – likely facilitated by Fc-receptor-mediated[Da Silva 2007] VLP uptake by DCs – has been achieved by pre-incubation of the VLPs with antibodies elicited against capsids of the proteins used to package the replicons. And this amplification is seen in dendritic cells from different donors and for different reporter and vaccine RNA genes. Preliminary in vivo experiments involving vaccination of mice with antigen-replicon VLPs show a small but significant generation of antigen-specific T cells that are doubly positive in their induction of IFN and TFN cytokines.

The modest T-cell response reported here provides a proof-of-principle for our RNA replicon virus-like particle vaccine platform. In contrast with plasmid-DNA and viral-vector delivery systems, in particular those involving lentiviruses, adenovirus, and adeno-associated virus, there is no need for genetic information to access the nucleus of the host cell and no possibility of integrating genes into the DNA of the host cell. There are also no viral-specific immune responses that interfere with efficacy of vaccine boosts. mRNA vaccines have none of these drawbacks because they are translated directly in the cytoplasm and gene expression is only transient. They also have the advantage that they act simultaneously as adjuvants, because they interact with pattern-recognition receptors that elicit innate immune response enhancing the

maturation of DCs and induction of adaptive immune response. Further when combined with the right RNA replicase gene, the mRNA vaccine is amplified strongly before being translated, resulting in a high level of in situ protein expression. Several mRNA replicon vaccines of this kind have been reported (see the recent review by Maruggi, et al.[Maruggi 2019], and references contained therein), but ours is the first in which the RNA is in vitro reconstituted in a perfectly monodisperse, RNase-resistant, spherical protein shell, instead of being "packaged" in less-well-characterized complexes involving lipids, cationic polymers, or various combinations of these components. In addition, our virus-like particles can be conjugated with ligands that enhance their uptake by targeted dendritic cells, and additional RNA genes included to further enhance dendritic cell activation and subsequent T cell priming.

The two essential ingredients of our approach derive from the special properties of two different non-mammalian viruses: (1) the insect virus Nodamura provides the self-replicating RNA molecule (with its associated RNA-dependent RNA polymerase) into which genes of interest (such as the OVA antigen) can be inserted; and (2) the plant virus CCMV provides the capsid protein ensuring the *in vitro* packaging of these replicons and consequent uptake by DCs. Nodamura is remarkable insofar as its RdRp functions in mammalian cells and is short enough to be packaged by CCMV CP, even after inclusion of interesting reporter genes or model antigens. And CCMV is remarkable insofar as its purified CP is uniquely capable of completely packaging, by spontaneous self-assembly, essentially any RNA sequence as long as its length does not exceed about 4000nt.

ACKNOWLEDGEMENTS

We thank Drs. Leonid Gitlin and Raul Andino (UCSF) for their generous gift of the plasmids from which we engineered our reporter-gene Nodamura replicons, and for many extremely helpful discussions. We are also grateful to Dr. Rees Garmann (Harvard) for the electron microscope image and VLP size histogram shown in Figure 11B.

3.6 Materials and Methods

Reagents

Recombinant human GM-CSF and IL-4 were purchased from R&D Systems (Minneapolis, MN, USA). PE-labeled antibodies (Abs) against human CD80, CD86 and MHC II were from BD Pharmingen (San Diego, CA, USA) and isotype control Abs from R&D Systems (Minneapolis, MN, USA). Complete Freund's Adjuvant, Incomplete Freund's Adjuvant and Lipopolysaccharide (LPS; Escherichia coli, O111:B4) were obtained from Sigma (St Louis, MO, USA). The goat anti-mouse HRP-conjugated secondary ab (goat anti-mouse IgG-HRP SC-2005, Lot # D1614) was purchased from Santa Cruz Biotechnology (San Diego, CA, USA). The BioFXr TMB super-sensitive one-component HRP microwell substrate was from SurModics (Minneapolis, MN, USA) and the BioStack Microplate Stacker from BioTek Instruments (Winooski, VT, USA). RPMI-1640 (-L glutamine) and L glutamine were from Thermo Fisher (Waltham, MA, USA) and heat-inactivated fetal bovine serum (FBS) from Sigma (F4135-500, 15H095H1).

BHK Cell Culturing and Transfections

BHK-21 cells were cultured in medium composed of high-glucose DMEM medium with 10% FBS and penicillin/streptomycin. The incubation conditions were 37˚C and 5% CO_2. Standard passaging was performed with the involvement of PBS for washing, and 0.25% trypsin-EDTA for cell detachment. All the above cell culturing reagents and medium were from ThermoFisher. The cells were passaged to 60-90% confluence in 24-well cell-culture-treated plates and, prior to transfection, were washed with PBS. For each well, 5 µl of lipofectamine-2000 (Thermo Fisher) was diluted with Opti-mem medium (Thermo Fisher) before mixing with 0.5 µg of RNA that is also diluted to an equal volume in Opti-mem. Since the replicon is so effective, the masses of mRNA prescribed in the lipofectamine-2000 manufacturer's protocol for the replicon were making the cells sick. By diluting the replicon RNA, a similarly large luciferase activity compared to higher concentrations of transfected mRNA is observed (especially when compared to the equimolar luciferase mRNA). Masses of 12.5 ng of luciferase replicon mRNA and 3 ng of luciferase mRNA were diluted with uncapped carrier RNA of similar length up to 0.5 µg, in order to achieve a similar number of liposomes per transfection.

Luciferase Assay

The luciferase assay was performed using the *Renilla* Luciferase Assay System from Promega (Fitchburg, WI, USA), and activity was measured using a Monolight 2010 luminometer. Cells were washed with PBS before directly lysing using passive lysis buffer and a cell scraper. 100 µl of *Renilla* luciferase assay reagent was added to a polycarbonate tube and luminescence was measured with 10 seconds of integration and a 2-second delay directly after adding 20 µl of cell

lysate and mixing. Luciferase activity was performed in biological and assay duplicates for each time point.

Cloning of Replicon Constructs

The plasmids constructed for these experiments were derived from plasmids kindly provided by Dr. Leonid Gitlin, from his work in Prof. Raul Andino's lab at UCSF. Synthesis was performed from Nodamura virus strain Mag115, cDNA using random hexamers and SuperScriptIII (Invitrogen). The eYFP-replicon used was the same construct entitled pNoda-B1-FPG in their paper. The luciferase-replicon and OVA epitope-replicon plasmids were constructed from their construct pNoda-PolT2A-GFP. The luciferase gene for the luciferase-replicon was PCR-amplified from the plasmid pSP64-Ren Luc-Poly(A) – denoted as SP6 luciferase in Figure 10. pSP64-Ren Luc-Poly(A) has the Renilla luciferase open reading frame from pRL null (Progema), cloned into the XbaI site of pSP64 Poly(A) vector (Promega). The gene was PCR-amplified gene using Phusion High-Fidelity Polymerase (NEB), and included NdeI and AgeI restriction sites for insertion into the corresponding sites of the pNoda-PolT2A backbone. The construction of the OVA epitope-replicon plasmid began with ordering complementary oligos encoding the SIINFEKL peptide sequence from IDT. These oligos have flanking NheI and XbaI sequences, as well as an overhanging 'A' nucleotide at the 3' ends to allow for 'TA-cloning' into a pGEM-T Easy Vector (Promega). When the pGEM vector with inserted SIINFEKL sequence is digested with a combination of either ScaI/XbaI or ScaI/NheI, the remaining XbaI and NheI sites are complementary. This process is repeated to result in a 4X tandem OVA epitope sequence, which is then cloned into the pNoda-PolT2A backbone by the same methods as the luciferase-replicon.

Synthesis of Replicon mRNA-VLPs

The replicon constructs were linearized with XbaI and subsequently purified using QIAquick PCR purification columns from Qiagen (Valencia, CA, USA). The linearized DNA was transcribed with T7 RNA polymerase. The buffer composition of the reaction was 40 mM Tris pH 7.5, 25 mM $MgCl_2$, 4 mM µl DTT, and 2 mM spermidine. The rNTP concentration was 7.5 mM. Incubation was for 3 hours at 37°C, followed by a 30-minute incubation with turbo DNase at the same temperature. The resulting RNA was purified using the RNeasy mini kit from Qiagen, and then capped using the Vaccinia Capping System from New England Biolabs (Beverly, MA, USA). This process added a 7-methylguanylate cap structure to the 5' end of RNA in the presence of the capping enzyme, reaction buffer, GTP, and the methyl donor, SAM. The *in vitro* transcription and capping were both done in the presence of RNase inhibitors to preserve the RNA, and the capping mixture was again purified by an RNeasy mini column (Qiagen). Generating VLPs first involves isolation of CCMV CP from CCMV. The CCMV was purified from infected Cowpea plant leaves. To purify the CP, the virion was loaded into 6 kDa dialysis bags, and dialyzed in disassembly buffer (500 mM calcium chloride, 50 mM Tris-HCl pH 7.5, 1 mM EDTA, 1 mM DTT, and 0.5 mM PMSF). After dialysis, the disassembled CP-RNA mixture was pipetted into polycarbonate tubes and centrifuged in a TLA 110 rotor at 95k for 2 hours. (This dialysis step and the three described immediately below – for CP purification, CP-RNA binding, and capsid formation – were each carried out for 6 hours at 4°C.) Fractions were taken after centrifugation, and a threshold A260/280 ratio of 0.6 was used to verify that they did not contain RNA. The capsid protein was dialyzed into Buffer B (1 M NaCl, 50 mM Tris-HCl pH 7.2, 1 mM EDTA, 1 mM DTT, and 1 mM PMSF). After determining the CP concentration with a Nanodrop Spectrophotometer, CP was combined with mRNA at a ratio of

12.9 µg of CP to 3µg mRNA (representing the minimum excess of CP necessary for complete encapsidation of mRNA) in buffer B but without DTT or PMSF, for a total volume of 100µl. This mixture was then dialyzed into RNA Assembly Buffer, RAB (50 mM NaCl, 50 mM Tris-HCl pH 7.2, 10 mM KCl, 5 mM $MgCl_2$, and 1 mM DTT), after which the pH was dropped to form capsids by dialyzing into Virus Suspension Buffer (50 mM Sodium Acetate, 8 mM Magnesium Acetate). Finally, the sample was transferred to RAB without DTT in order to have a VLP sample at the necessary neutral pH for biological experiments. Once VLPs have been verified (methods for which are described in the following two sections), the mg/ml concentration of VLPs is measured using the Nanodrop by dividing the 260nm absorbance by 5.8, the same factor used when determining the concentration of purified virus. Because of the small excess of CP used for complete packaging of RNA, the recovery of VLP mass is about 80% of the total mass of mRNA and CP used in the assembly.

Verification of Assembly

After assembly, the first step to verify the formation of homogeneous VLPs is agarose gel electrophoresis. A native agarose gel was run at 50 V for 1.5 hours, with the running buffer and the 1% agarose gel being made of 100 mM Sodium Acetate and 1 mM EDTA; the staining is with ethidium bromide. For reference, wild-type CCMV virion is included in a separate lane – the middle, in Fig. 4A. The assembly mix is treated with RNase and loaded directly onto the gel (rightmost lane): the reconstituted VLPs run more slowly because of excess protein adsorbed onto their capsids; a small (40%) excess of capsid protein has been used to guarantee complete packaging of all the RNA, and it binds to the negative exteriors of the self-assembled VLPs

through its cationic N-terminus[Cadena-Nava 2012, Garmann 2014a, Garmann 2014b, Garmann 2016]. VLP formation from in vitro assemblies has also been verified directly in bulk solution by sucrose gradient analysis (see our earlier study of VLPs involving the same lengths of RNA[Garmann 2014b] – in particular Fig. 3 there), where we compare the relative sedimentation profile peak positions for VLPs, wild-type virions, and virions plus excess protein and correlate them with the corresponding band positions in the electrophoretic gels.

Electron Microscopy

The preparation of well-formed intact VLPs was confirmed by negative-stain electron microscopy. 6 µl of VLPs is applied to glow-discharged copper grids (400-mesh) coated with Parlodion and carbon. After 1 min, the solution is blotted with Whatman filter paper. 6 µl of 1% uranyl acetate is then added to the grid. After 1 min, the excess uranyl acetate is removed by blotting. The grids are stored overnight in a desiccator and analyzed with a JEM 1200-EX transmission electron microscope equipped with a wide-angle (top mount) BioScan 600-W 1×1K pixel digital camera operated at 80 keV. The diameter of the VLPs is estimated by taking the geometric mean of two orthogonal measurements of the capsids obtained with ImageJ (U.S. National Institutes of Health) software from recorded images. The diameter of 100 VLPs is measured in this way and compared to the diameter of wtCCMV that had been previously imaged.

Generation and culture of monocyte-derived DCs

To generate immature DCs, $CD14^-$ monocytes negatively isolated from human peripheral blood mononuclear cells were cultured in a 24-well plate (1.0×10^6 cells/ml/well) with RPMI-1640 (-L glutamine) medium containing 1 × L glutamine and 10% heat-inactivated fetal bovine serum for 5 days. The donors were anonymous, but the number designation of PBMC for the figures included in this article are as follows: figure 12 Ai and Aii – A5394, figure 12 B – A5154, figure 13 – A5167, and figure S2 – A5167. Culture medium was supplemented with recombinant human GM-CSF (10 ng/mL) and recombinant human IL-4 (10 ng/mL).

Pulsing of dendritic cells

On day 5, immature DCs (1.0×10^6 cells/ml/well) were pulsed with naked eYFP mRNA, CCMV VLPs carrying eYFP mRNA, naked eYFP replicon mRNA, CCMV VLPs carrying eYFP replicon mRNA, CCMV VLPs carrying OVA-replicon mRNA, OVA-replicon-carrying CCMV VLPs pre-incubated with anti-CCMV VLP abs or naïve serum abs, and eYFP-replicon-carrying CCMV VLPs pre-incubated with anti-CCMV VLP abs or naïve serum abs. DCs stimulated with LPS and media were used as a positive and negative control, respectively. Following 24 hours of incubation, expression of activation markers for human DCs such as CD80, CD86 and MHC II was analyzed using flow cytometry.

Mouse immunization

C57BL/6Tac mice between 6-8 weeks of age were purchased from Charles River Laboratories (Wilmington, MA). They were immunized subcutaneously with CCMV VLPs containing a non-

translated RNA (20 µg/per mouse/per immunization) on weeks 0, 2, and 4 using Complete Freund's Adjuvant for priming and the subsequent boost with Incomplete Freund's Adjuvant. The animal use protocol was approved by IACUC committee of Boehringer Ingelheim Pharmaceuticals. Serum samples collected one week after the 3rd immunization were evaluated by ELISA to determine the antibody titer against CCMV VLPs. Pre-bleed was used as a negative control.

Enzyme-linked immunosorbent assay (ELISA)

To determine the end-point titers, CCMV VLPs were coated onto Immulon 2 HB 96-Well Microtiter plates (Catalog # 227, ImmunoChemistry Technologies, Bloomington, MN) at 0.5µg/mL using PBS overnight at 4 °C. Uncoated surface was blocked using phosphate-buffered saline (PBS) containing 3% Bovine Serum Albumin for 1 hr at 37°C. The plates were subsequently washed 5× with 0.05% Tween 20 in PBS. Mouse serum serially diluted (three-fold) in the blocking buffer was added to each well and incubated for 2 hrs at 37°C. The plates were washed 5×, and horseradish peroxidase (HRP)-conjugated secondary ab (goat anti-mouse IgG, 1:3000 dilution) was added to each well and incubated for 1 hr at 37°C. Plates were washed 5× and developed by adding 100 µl BioFXr TMB super-sensitive one-component HRP microwell substrate for 5 min. Reactions were stopped with 50 µl of 2 N H_2SO_4. Plates were read on a microplate reader (BioStack Microplate Stacker) at 450 nm. All experiments were performed in duplicate.

Quantitative PCR

The Power SYBR® Green Cells-to-CT kit was used for the detection of OVA and eYFP mRNA uptake by DCs. Briefly, the passively pulsed dendritic cells were washed twice with ice-cold 1 × PBS. RNALater (200 µl) was added to the well(s). The plate was sealed with PetriSEAL and placed at -80^{o}C. To isolate RNA, the plate was thawed rapidly and an equal volume of ice-cold 1 × PBS was added to the well(s). The plate was spun at 1400 rpm for 5 min at 4°C. The fluids were removed carefully and the cell layer was washed again twice with ice-cold 1 × PBS. The cells were lysed for 5 min at room temperature in 50 µl of Lysis solution supplemented with DNase I (all supplied in the Power SYBR® Green Cells-to-CT kit). The reactions were then stopped with 1/10 volume stop solution and left at room temperature for 2 min. 10 µl of the lysate was added to the reverse transcription reaction cocktail that contained 1× SYBR RT buffer with 1× RT Enzyme mix. The reaction was run at 37°C for 1 hr followed by a 5-min 95°C heat kill of the enzyme.

Four microliters of the reverse-transcribed material was added to 16 µl of gene-specific forward and reverse primers at 400 nM in the PowerSYBR Green PCR master mix. The samples were run using a Viaa7TM cycler (95°C for 10 min to activate the enzyme; 40 cycles of 95°C for 15 seconds and 60°C for 1 minute to amplify the sequence of interest). The CT values were generated by the Viaa7 program. Relative expression of the pulsed mRNA was calculated by finding the differences between pulsed mRNA CT values and the CT value for the ACTB housekeeping gene generated from the same cells by using the relation: RelExp = POWER (2 - (CT value)).

For quantifying luciferase RNA in BHK cells in the Figure 10 time course, a different qPCR approach was utilized. The transfected BHK cells were lysed using buffer RLT in the RNeasy mini kit from Qiagen. Before purifying with the standard RNeasy mini kit protocol, the lysate was passed through a QIAshredder column (Qiagen) in order to remove insoluble debris. After purification, the concentration was verified with a Nanodrop Spectrophotometer, and 1 µg was reverse transcribed using M-MuLV reverse transcriptase from NEB. The flanking luciferase qPCR primer was used to synthesize the cDNA. In order to quantify RNA number, a standard curve with known concentrations of luciferase replicon RNA from 100 pg to to 10 fg was assayed by qPCR using the standard protocol for SsoAdvanced Universal SYBR Green Supermix (Bio-Rad, Irvine, CA, USA). The concentration of the luciferase amplicon primers used was 200 nM. For the time course samples, 100 pg and 10 pg cDNA of the luciferase mRNA and replicon transfected cells were assayed by qPCR, respectively.

Mouse vaccinations

C57BL/6Tac female mice were provided by Taconic Denmark. The mice were transferred to the local AAALAC accredited animal facility at Boehringer Ingelheim RCV GmbH & Co KG at an age of 6-8 weeks, and immediately after arrival were allowed to adjust to conditions for at least 5 days before they were used for experiments. Standardized diet (PROVIMI KLIBA) and autoclaved tap water were provided *ad libitum*. Mice were group-housed (8 mice per cage) under pathogen-free and controlled environmental conditions (21 ± 1.5°C temperature, 55 ± 10% humidity) and handled according to the institutional, governmental and European Union

guidelines (Austrian Animal Protection Laws, GV-SOLAS and FELASA guidelines). Animal studies were approved by the internal ethics committee and the local governmental committee.

Two different vaccination schedules were tested. In the first scenario mice were vaccinated subcutaneous (s.c.) only once, with either buffer as control, with the Ova Protein (50µg), with the SIINFEKL Replicon (100µg), or with the VLP containing the SIINFEKL replicon (100µg). The volume of all applications was 100µL, and after one week the mice were euthanized and spleens were harvested for FACS analysis. In the second vaccination scenario mice were vaccinated with buffer as control or with buffer containing VLPs containing the SIINFEKL replicon RNA (100µg). The vaccinations were administered s.c. with a volume of 100µL for 3 consecutive weeks (q7d), and one week after the last injection the mice were sacrificed and their spleens were harvested for FACS analysis. In addition one C57BL/6Tg(TcraTcrb)1100Mjb/Crl (OT-1) mouse provided by Charles River Laboratories (France) and one C57BL/6Tac mouse were euthanized and their spleens harvested to collect T-cells as control for the FACS analysis.

In vitro stimulation and single-cell analysis by flow cytometry

Splenocytes from vaccinated and control mice were obtained by tissue homogenization followed by red blood cell lysis (ammonium-chloride-potassium lysis). Ovalbumin specific $CD8^+$ T cells, present in the cell suspensions, were stimulated with 8µg/ml of SIINFEKL(Ova 257-264, InvivoGen) and TEWTSSNVMEERKIKV(EMC microcollections) peptides together with 10µg/ml anti-CD28 antibody (BioLegend) for 6 hours. One hour after start of stimulation, a protein-transport-inhibitor cocktail (eBioscience), containing Brefeldin A and Monensin, was added to block cytokine release. Before surface-marker staining, dead cells were labeled with a

fixable viability stain and Fc receptors were blocked (TruStain fcX, BioLegend) to avoid nonspecific binding. Key surface markers were stained with fluorescently labeled antibodies, followed by fixation/permeabilization (BD Cytofix/Cytoperm Plus, BD Biosciences) and intracellular cytokine staining (FITC anti-mouse IFNγ and PE-Cy7 anti-mouse TNFα, eBioscience).

For immunophenotyping including the detection of H-2Kb/SIINFEKL specific CD8 T cells, spleens were dissociated using a spleen dissociation kit from Miltenyi biotec, together with a gentle MACS Dissociator. After red blood cell lysis, labeling of dead cells and Fc Receptor blockade, single cell suspensions were incubated with H-2Kb/SIINFEKL pentamer (ProImmune) for 30 minutes at 4 to 8^{o}C. After thorough removal of unbound pentamer, key surface markers were labeled fluorescently with specific antibodies.Flow data were collected with a BD LSRFortessa cell analyzer and further analyzed using FlowJo 10 and GraphPad Prism 7.03.

3.7 Supporting Information

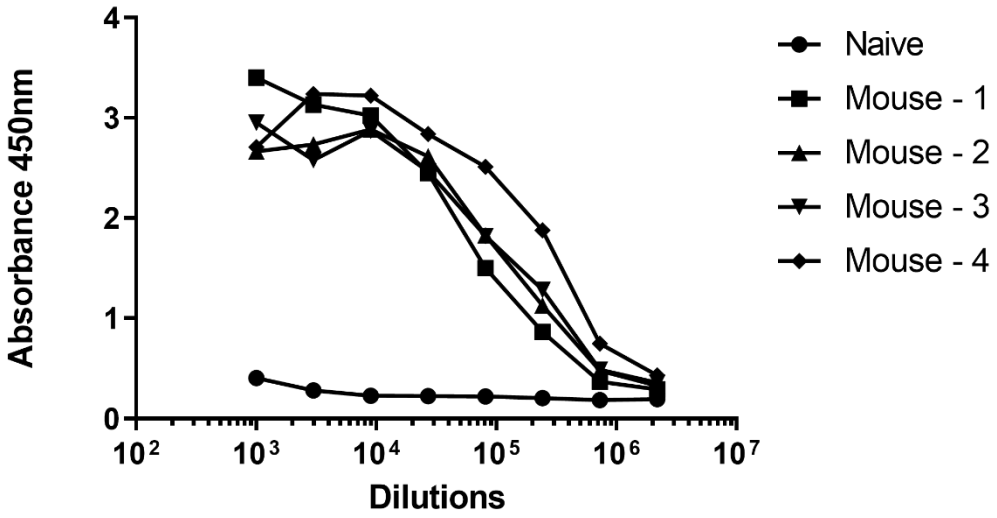

Figure S1. Antibody Titers. Four C57BL/6Tac mice were immunized subcutaneously with CCMV VLPs containing a non-translated RNA (20 µg/per mouse/per immunization) on weeks 0, 2, and 4. Sera were tested for binding to CCMV VLPs 1 week after the 3rd immunization. Pre-immune serum ("Naïve") was used as a negative control.

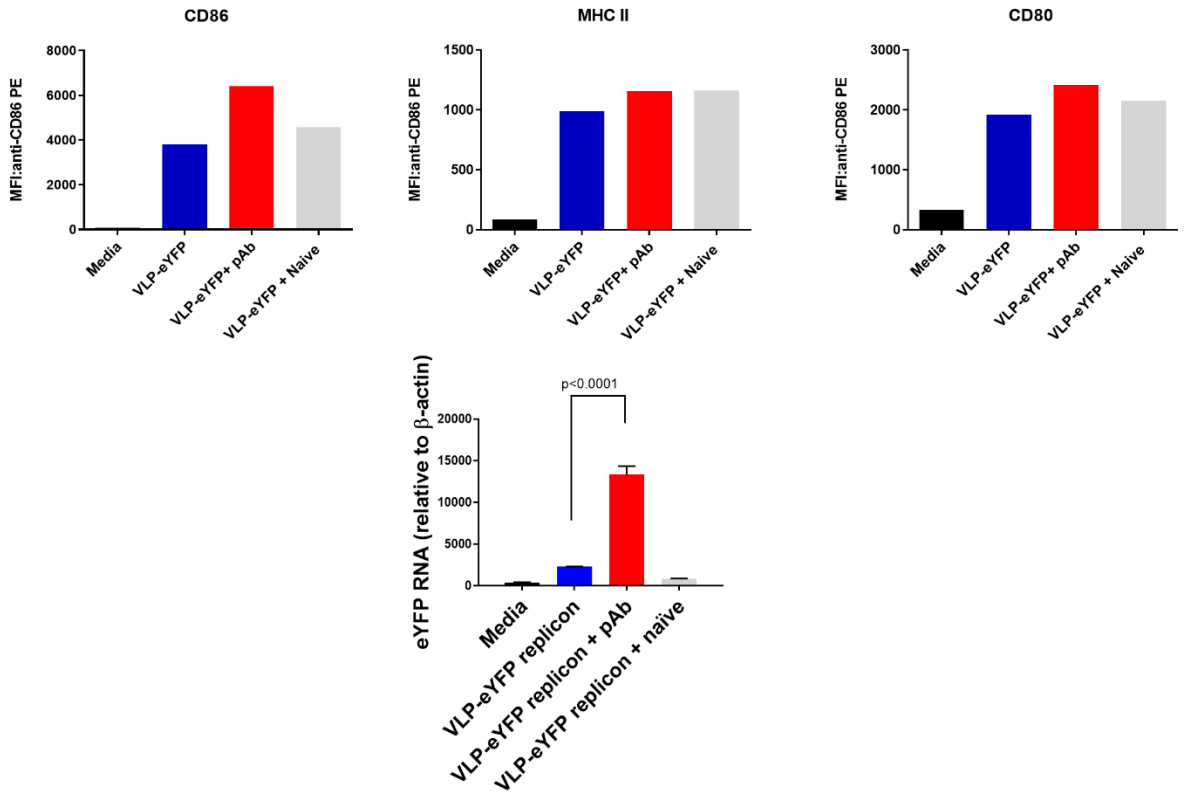

Figure S2. TOP: Expression intensity of activation markers on DCs treated with CCMV VLPs carrying eYFP-Replicon mRNA. The median fluorescence intensity (MFI) of CD86 (left), MHC II (middle) and CD80 (right) was determined for DCs treated with media only (black bars), CCMV VLPs carrying eYFP replicon mRNA (blue bars), and CCMV VLPs carrying eYFP replicon mRNA that have been pre-incubated with anti-CCMV VLP (red bars) antibodies or naïve antibodies (grey bars).

BOTTOM: RNA quantitative PCR (qPCR). DCs treated as above were lysed and eYFP-specific mRNA levels were determined by qPCR – note break in vertical scale. The p value was determined using a one-way Anova test.

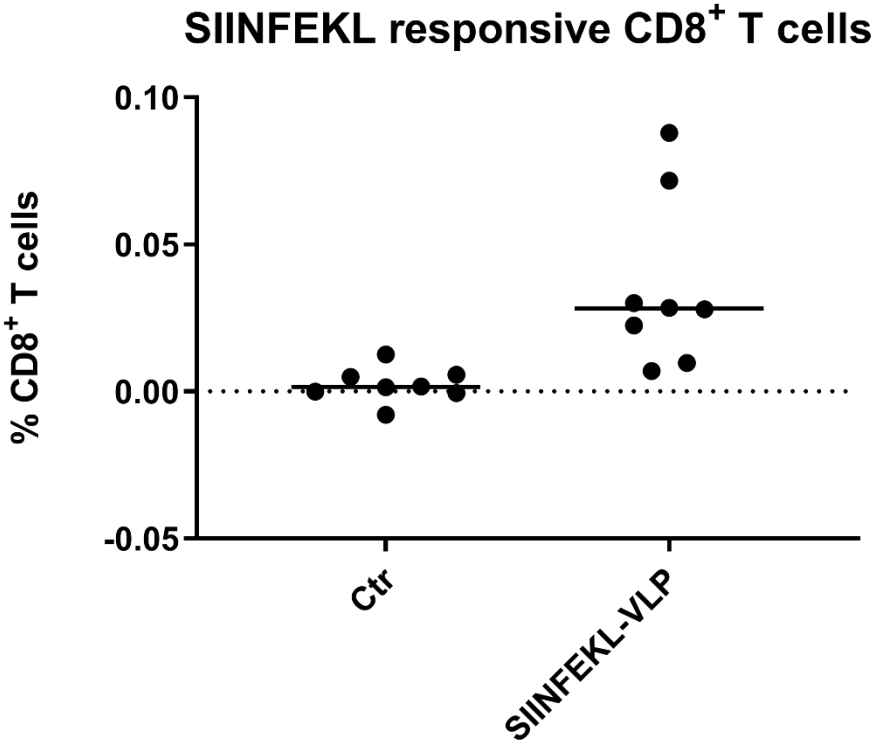

Figure S3. Cytokine production of SIINFEKL responsive CD8$^+$ T cells. T-cells were stimulated with SIINFEKL peptide for 6 hours. The amount of INF-gamma and TNF-alpha double-positive cells is shown as percentage of total CD8$^+$ T cells. Samples analyzed in this assay have been obtained from the same animal experiment described in Figure 14, with "Ctr" and "SIINFEKL-VLP" denoting the multiple vaccinations involving buffer-solution and OVA-replicon-VLP, respectively.

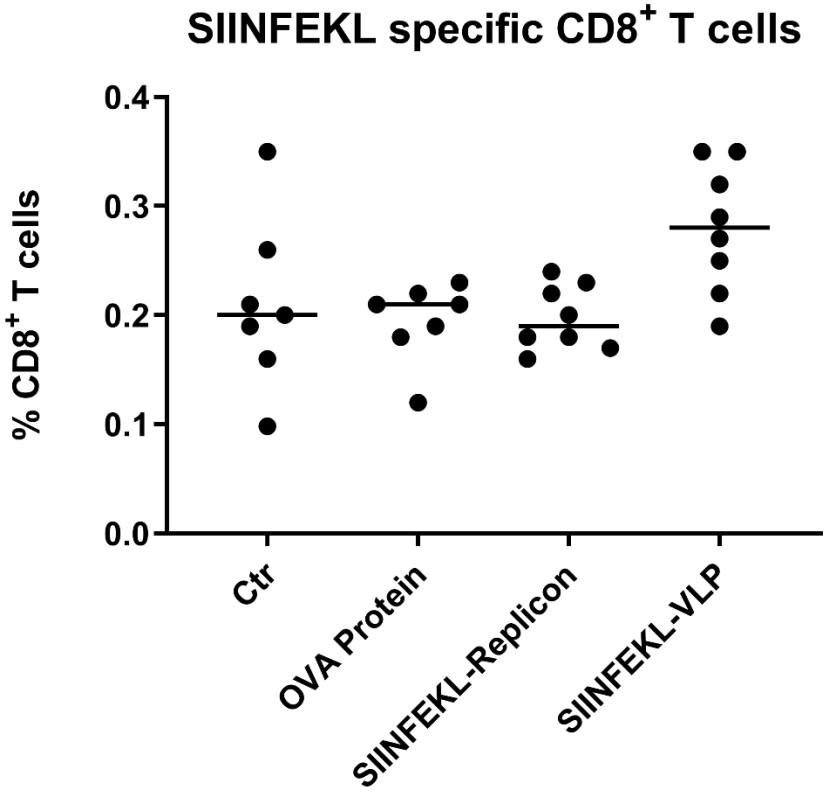

Figure S4. Low frequency of H-2Kb/SIINFEKL-specific CD8$^+$ T cells in mice vaccinated only one time. The fraction of SIINFEKL specific T-cells in spleen samples, collected one week following a one time only vaccination, was determined by flow cytometry. The graph shows scatter plots for single vaccinations with negative control ("Ctr", 100 µL of buffer solution) positive control (50 µg of "OVA Protein"), 100 µg of SIINFEKL replicon RNA and 100 µg of SIINFEKL-VLPs. The difference of less than 0.1% between the SIINFEKL-VLP outcome and that for the negative control is to be contrasted with the 0.4% difference found for the multiple-boost vaccination with the same VLPs (see Figure 14). To compare all groups an Anova test was performed together with a Dunnett's test to correct for multiple comparisons (p= 0.0484) between the "Ctr" and the "SIINFEKL-VLP" groups.

Chapter 4: Two-molecule replicon for co-delivery of replicon and large genes

4.1 Construction of dual replicated RNA molecules

Since RNA1 of *Nodamura virus* (NoV) is already about the size (3000nt) of each genomic RNA packaged into CCMV, there is a limitation on the size of the GOI inserted. Our lab has demonstrated that in vitro assemblies of RNA above 4500 nt in length result in a major population of capsid multimers, i.e., two or more T=3 capsids sharing a single RNA molecule These multimers are more susceptible to RNase degradation, so maintaining single T=3 capsids requires packaging RNA between about 2000-4500 nts in length, which limits the size of the GOI we can add and/or the number of added GOIs.

A promising avenue to allow for amplification of larger GOIs involves leaving RNA1 of NoV unchanged, and inserting the GOI into the RNA2 of NoV which is also replicated. A previous study[Rosskopf 2012] has shown that by preserving the untranslated regions of RNA2, even while substituting the capsid protein open reading frame with GFP, there is still replication of RNA2. These authors transfected the plasmids encoding combinations of full-length RNA1 and varying regions of RNA2 into yeast. From their experiments they identified a 24-nt stem loop near the 3' end that is necessary for replication. While demonstrating replication with just the sequence of the untranslated 3' end that includes the stem loop, they showed that preserving in addition some of the sequence for the capsid protein gene (for a total of 236 nts) resulted in more replication.

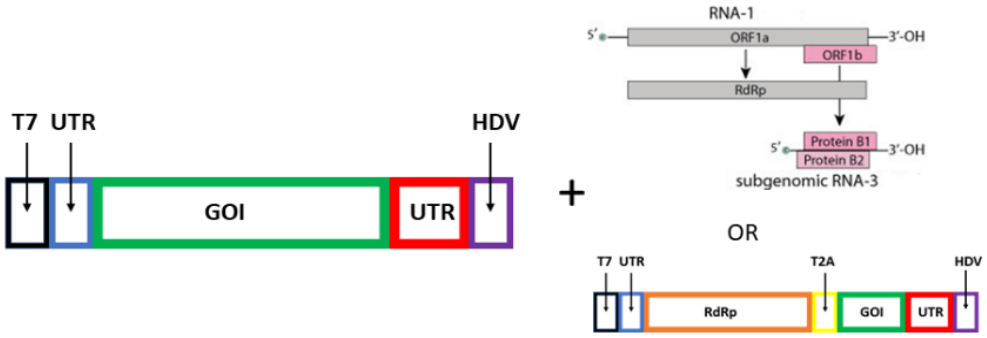

Figure 15: Schematic of a proposed two-molecule system for amplification of a gene inserted into RNA2 of NoV. LEFT is the RNA2-GOI, and RIGHT shows either a WT RNA1 molecule or GOI-RdRp molecule that would help to replicate the complementary RNA2 molecule.

4.2 Reporter gene studies of two-molecule replicons

The replicon-VLP strategy involves an RNA1, either wild-type or with a single-molecule replicon containing a desired gene, and a separate RNA2-GOI. This RNA2 construct – depicted in figure 15 - includes a GOI replacing the capsid protein gene of *nodamura*, and to promote replication this gene is flanked by the 5' untranslated region (UTR) 17 nts from the beginning and 236 nts (which includes the end of the capsid gene and the whole 3' UTR) from the end of RNA2. Co-transfection of wild-type RNA1 with RNA2 modified to include luciferase revealed greater expression than either luciferase mRNA or the modified RNA2 alone (figure 16).

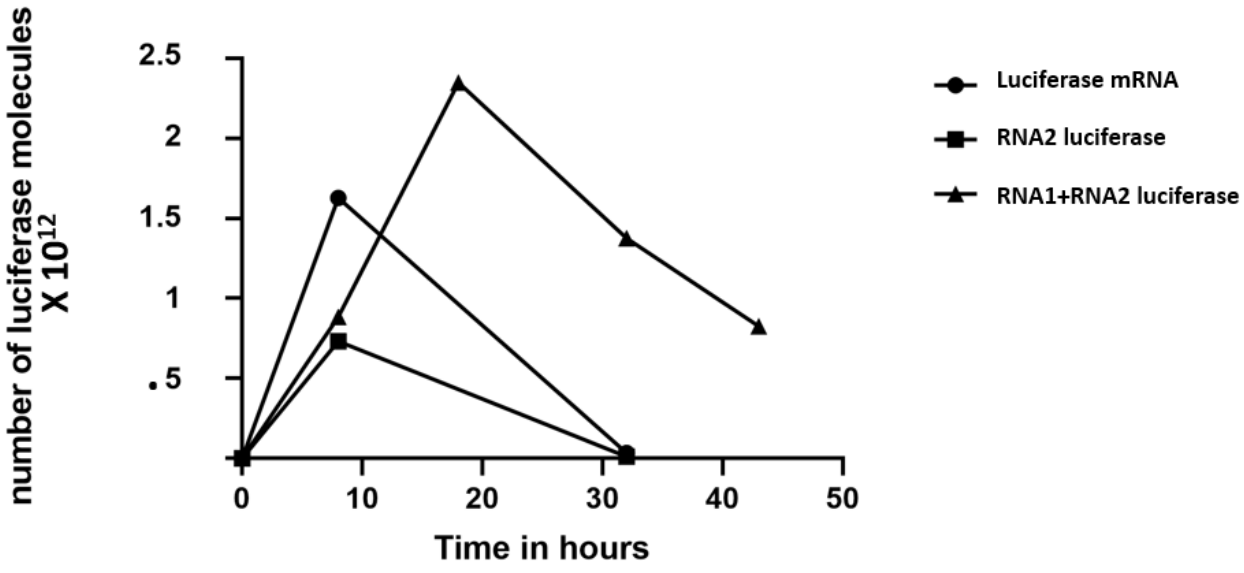

Figure 16: Time course of luciferase expression in BHK 21 cells. Luciferase mRNA, RNA2 luciferase, or WT RNA1 + RNA2 luciferase were all separately transfected with lipofectamine in equal copy number.

Although we have shown that the protein expression when the luciferase-RNA2 is coupled with wild-type (WT) RNA1, further experiments need to be performed to determine its potential for therapeutic applications. As in the experiments in which the single-molecule EYFP-replicon was utilized to track the replication cycle of the replicon and health of transfected cells, a fluorescent protein can be inserted into RNA2 to observe a similar phenomenon for the two-molecule replicon system. An EYFP-replicon can be co-transfected with an RNA2 encoding a different fluorescent protein (mCherry fluorescent protein), in order to concurrently visualize protein expression from both molecules. This method would not only allow verification of each molecule being expressed within a certain cell, but also might demonstrate colocalization of the complementary molecules. The above experiment with two fluorescent genes can be performed

in vitro by either transfecting each mRNA into BHK cells, or incubating each VLP with dendritic cells (possibly at separate times).

This two-molecule strategy may hold promise for a vaccine system. Eventually, a two-molecule ovalbumin system would probably involve separately packaged WT RNA1 and antigen-RNA2. Since we have demonstrated that an ovalbumin epitope-repeat in RNA1 can elicit a killer T cell response, this single-molecule replicon can be paired with an RNA2 containing either an additional antigen and/or adjuvant to boost the immune response.

The considerations for keeping the length of gene inserted into RNA1 short enough to keep it packageable into a single T=3 capsid, or putting the gene into RNA2 apply as well to maintaining a preferred size of RNA2. Many genes encoding useful antigens or adjuvants are in the range of 1000-1500 nts, which results in an RNA2 molecule that is less than 2000 nts. For assemblies of RNA lengths around 2000 nts and below, the populations of capsids are heterogeneous and show a significant portion of capsids that are 6-10 nm smaller (presumed to be T=2 capsids) than wild-type T=3 virus. In order to maintain an optimal length for packaging the RNA2, one option is to make a dual protein construct. With two copies of genes of around 1000-1500 nts, along with the untranslated replication elements, one achieves an ideal size (~3000nt) for assembly. One approach for including two genes involves making a fusion protein construct that has the same self-cleaving T2A peptide as in the single-molecule replicon, to separate the two protein products. Another option is to separate the two genes by an internal ribosome entry site (IRES). This is an RNA element that would allow for separate translation of the second gene in RNA2 in a cap-independent manner. While the fusion protein would have one read-through translation event to generate both proteins, the IRES-RNA2 would involve separate ribosomes binding and initiating translation events at the 5’ capped end and at the IRES.

One candidate gene for the use of a two-molecule system as part of a viral vaccine is the HIV envelope protein glycoprotein 120 (gp120). HIV gp120 is a widely studied envelope protein involved in viral entry into immune cells via binding of the CD 4 receptor[Kwong 1998]. The length of the gp120 gene is ~1400 nt, which is too long to insert into RNA1 of NoV and still have it packaged into single T=3 capsids. When inserted into RNA2, the total length is below 2000 nt. To make a molecule long enough for efficient packaging into a T=3 structure, we explored generating a fusion protein. This fusion protein could include a second copy of gp120, some other antigen, or even adjuvant. To test the efficacy of a fusion protein in an RNA2 molecule, we cloned an RNA2 that included the gp120 gene separated from the eYFP gene by a T2A peptide. From the fluorescence exhibited after 20 hours, we demonstrated that the second gene can be translated (figure 17). In addition, an analogous transfection was performed using equal numbers of single-molecule eYFP-replicon and RNA2 ENV-eYFP. Corroborating the luciferase results of single-molecule (figure 4) and two-molecule transfections (figure 16), we see that the protein expression is less robust in the two-molecule scenario (figure 16). This appears to be another possible method for attenuation of the replicon in gene-delivery efforts where the health of the target cell is a concern.

A

RNA2 Env-eYFP + replicon **Brightfield image**

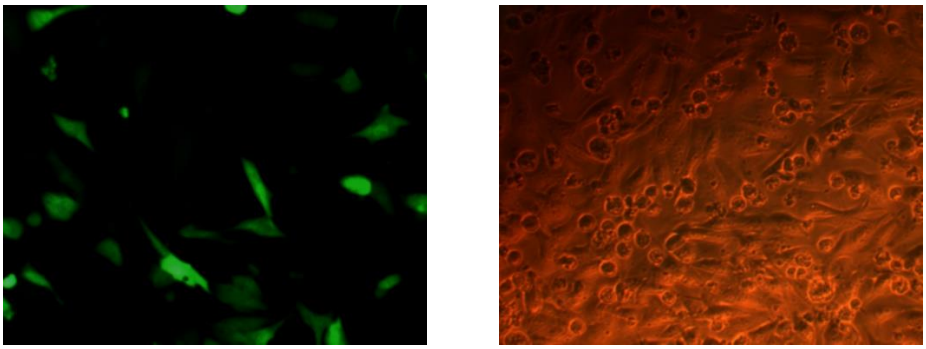

B

eYFP-replicon **Brightfield image**

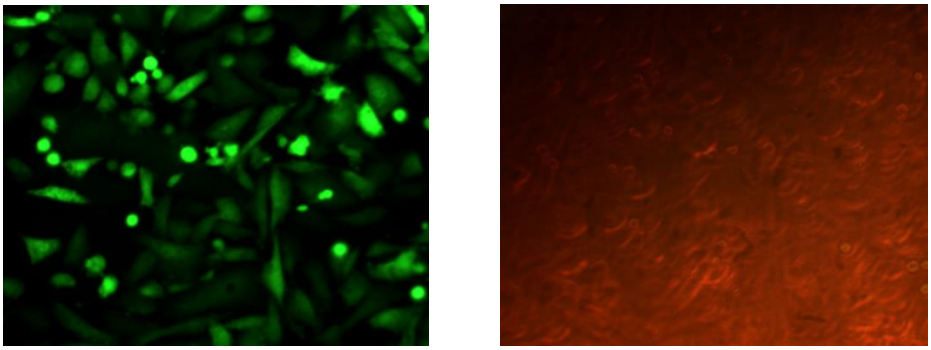

Figure 17: Fluorescence and brightfield microscope images of BHK 21 cells transfected with replicon after 20 hours. A shows the fluorescence exhibited by a lipofectamine transfection of WT RNA1 and an RNA2 molecule containing the fusion HIV envelope protein and eYFP genes separated by a T2A self-cleaving peptide. **B** shows a transfection done in parallel with an equal copy number of eYFP-replicon.

Chapter 5: Generation and characterization of cysteine mutant CCMV

While having a protected mRNA cargo is important for gene delivery, there is still a question of the replicon-VLP making it into the proper cells. In the vaccine approach of delivery to dendritic cells as a means of eliciting a specific killer T cell response, the necessity for specific targeting is lessened because the dendritic cells are primed to endocytose virus-like capsids. In other gene delivery scenarios, targeting specific cell types or cancerous cells may be desired. One approach for targeting a VLP to cells is conjugation of antibodies (complete or partial) to the capsid surface. In order to perform a conjugation to CCMV, there is a benefit to modifying the CP.

5.1 Site-directed mutagenesis of CCMV cDNA plasmid

The most commonly used amino acid residues for conjugation to antibodies are lysine and cysteine. One method of labeling proteins utilizes the primary amines that exist in the side chains of lysines. CCMV has several surface-exposed lysines present in each capsid protein subunit, and the Gelbart/Knobler group has used NHS esters (N-hydroxysuccinimide esters) conjugated to fluorophores for labeling of capsids. An effect observed from this NHS ester-mediated fluorophore labeling is a decreased ability of capsid disassembly with greater amounts of labeling. CCMV does not have any surface-exposed cysteines, so there has been interest in introducing a cysteine for potential functionalization/labeling of capsids. A Michael-addition of

thiol to a maleimide is commonly used for bioconjugation, and two FDA-approved antibody-drug conjugates – Brentuximab vedotin and Trastuzumab emtansine – contain a thiol-maleimide adduct (Fontaine 2015). A group at Montana State University introduced cysteines onto each CCMV CP subunit to form a 2D-array on a gold surface utilizing the exposed thiols (Douglas 2003). A single labeling site on each CP subunit can be obtained by site-directed mutagenesis, thus controlling the amount of eventual conjugation. Furthermore, one can do a mixed assembly of cysteine-CP with wild-type CP to further limit the number of accessible sites for thiol-maleimide labeling.

To this aim we set out to introduce a cysteine into each CCMV CP by a method similar to the one employed by Douglas, et al. They used site-directed mutagenesis to change residue 163 from alanine to cysteine. Our group has plasmids which contain cDNA clones of RNA1, RNA2, and RNA3 generated by the Ahlquist group (reference needed). For the site-directed mutagenesis, primers were designed that anneal to both strands at residue 163 of RNA3's cDNA plasmid (named PCC3). The whole plasmid is amplified by PCR, now incorporating the amino acid change to cysteine present in the primer sequences. The PCR mixture is then digested by DpnI, which digests the parental DNA due to methylation during its E. Coli expression. After digestion, the mutated molecules are transformed into competent E. Coli cells, which will repair the nick formed during PCR. As with any cloning, colonies are grown up and the sequence is verified to ensure successful mutagenesis of A163C.

5.2 Transfection and purification of CCMV from cowpea plants

The plasmids containing cDNA of RNA1, RNA2, and RNA3 with a A163C mutation, were linearized at the XbaI site. Then they each underwent capped transcription, and were purified. In a protocol similar to that used for infection of cowpea plants, leaves were punctured by a microchip and a solution containing an equal amount of each mRNA was pipetted onto them and scraped with the pipette tip. After a week, classic mottling indicating infection was observed. After two weeks, the leaves were harvested, but the amount of virus in these few leaves was not enough for a purification. So the leaves were crushed in expectation that cysteine-modified CCMV could be released into a solution that could be used to infect more cowpea plants by the same means. These latter plants also displayed mottling, and two weeks after infection the leaves were harvested.

The procedure for purifying the cysteine-mutant virus was essentially the same as for wild-type CCMV. This involves taking infected leaves stored at -80 ˚C and crushing them with a mortar and pestle in a low pH, high molarity sodium and magnesium acetate buffer called virus extraction buffer. The crushed leaf mixture was then stirred with an equal volume of chloroform, then centrifuged to isolate the virus-containing aqueous solution. The virus was pelleted by ultracentrifugation, with aid of a sucrose cushion layer. These pellets were resolubilized in a 10-times-more-dilute buffer than virus extraction buffer, called virus suspension buffer. This solution was pipetted on top of a 10-40 percent sucrose gradient, formed by a freezing-then-thawing of 25 percent sucrose-VSB. Rayleigh scattering allows the band in the gradient containing the virus to be seen, allowing it to be pipetted. At this point we observed something different from purifications of wild-type virus. Instead of a single blue virus band, multiple bands

were observed, which we speculated are associated with different clusters of CCMV formed from disulfide bridges due to the cysteines on the capsid surface. When samples of the cysteine-mutant CCMV were run on an agarose gel next to wild-type, the band for A163C CCMV ran a bit faster than wild-type. This may be due to the isoelectric point being slightly changed when the nonpolar alanine is substituted for the polar cysteine amino acid. No additional bands were visualized in the gel for A163C CCMV, unlike in the sucrose gradient.

Although we established the above differences in the cysteine mutant, we wanted visual confirmation of the formation of capsids and the incorporation of 180 cysteine groups. It is well-known that thiols form a nearly irreversible bond to gold, so evidence of gold-labeling would confirm that unique cysteines have been added to the capsid surface. With the help of Dr. Christian Beren, conjugation of gold nanoparticles to the cysteines was undertaken. The protocol involved incubating citrate-stabilized 5-nm gold nanoparticles with an excess of cysteine-CCMV in a neutral pH phosphate buffer. This mixture is centrifuged at 13000 rpm, which is fast enough for only the gold nanoparticles to pellet. This pellet is resolubilized and imaged by negative-stain electron microscopy (EM). Gold particles were observed associated with the properly sized and ordered virus capsids – as seen in figure 18. While there are 180 potential sites of gold-thiol binding on cysteine-mutant CCMV, we only observed a few gold particles bound to each capsid. Since our aim for this experiment was only to confirm the introduction of surface-exposed cysteines to CCMV, the clustering of gold particle onto the virions was sufficient to confirm the presence of cysteines.

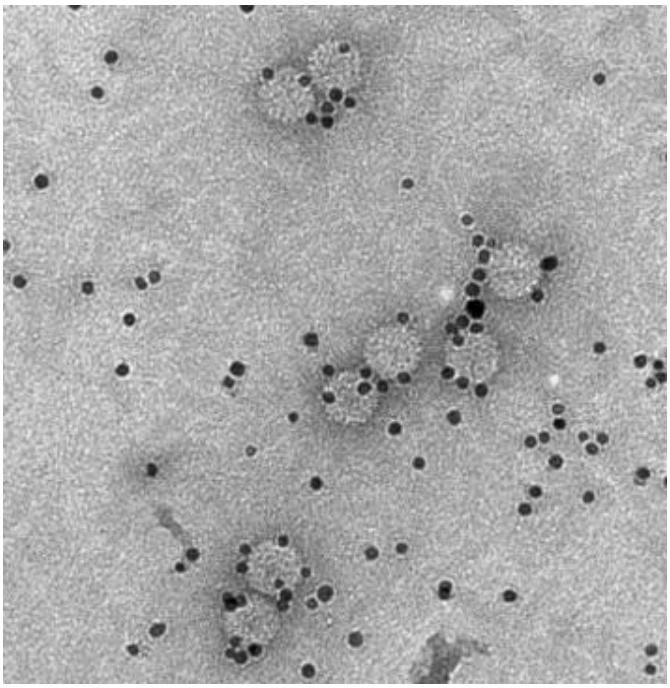

Figure 18: Electron micrograph of Cysteine-mutant CCMV labeled with 5-nm citrate-coated gold nanoparticles.

5.3 Self-assembly of cysteine-mutant CCMV alone and with WT capsid protein

Experiments were done to see if the cysteine-mutant CCMV CP (which we will refer to as CP*) can be used to self-assemble around RNA. Dissassembly of the cysteinylated mutant virions by dialysis into a high calcium buffer, followed by ultracentrifugation, successfully separated the CP* from viral RNA. Assembly was carried out using the same mass ratio – 4.3:1 CP:RNA – known for wild-type CP to fully encapsidate RNA. Lane 3 in the gel in Figure 19 shows that the CP* is able to fully encapsidate BMV RNA1 (B1 RNA). The CP* assemblies contribute a band that runs faster than WT assemblies (lane 6), as was the case for cysteine-

CCMV and wild-type CCMV. Again, this may be due to the isoelectric point being slightly changed by substitution of alanine to cysteine. In lane 3, we observe incomplete packaging of the B1 RNA, because the 2.8:1 CP*:RNA mass ratio is sub-stoichiometric for complete assembly. The appearance of the relatively smeared band of lane 2, located intermediate between the fully assembled (lane 3) and naked RNA (lane 5), is similar to that observed with WT CP assembly mixtures that include a sub-stoichiometric amount of CP[Garmann 2014].

One consideration when generating cysteine-CCMV is that purification yield about 3-4 times fewer CP less than wild-type from an equal mass of infected leaves. For this reason, and as another means to control the amount of labeling of CCMV, we attempted assembly using a mixture of CP and CP*. The single band in lane 7 resulting after an assembly with a 50-50 mixture of CP and CP* indicates well-formed particles. Also, the position of the band intermediate between those for the assemblies using either WT CP (lane 6) or CP* (lane 3) demonstrates that both forms of CP are incorporated into each VLP. If WT CP and CP* separately packaged individual RNA, we would see a band running in line with the slower WT CP assembly (lane 6), and a band in line with the faster migrating CP* assembly (lane 3).

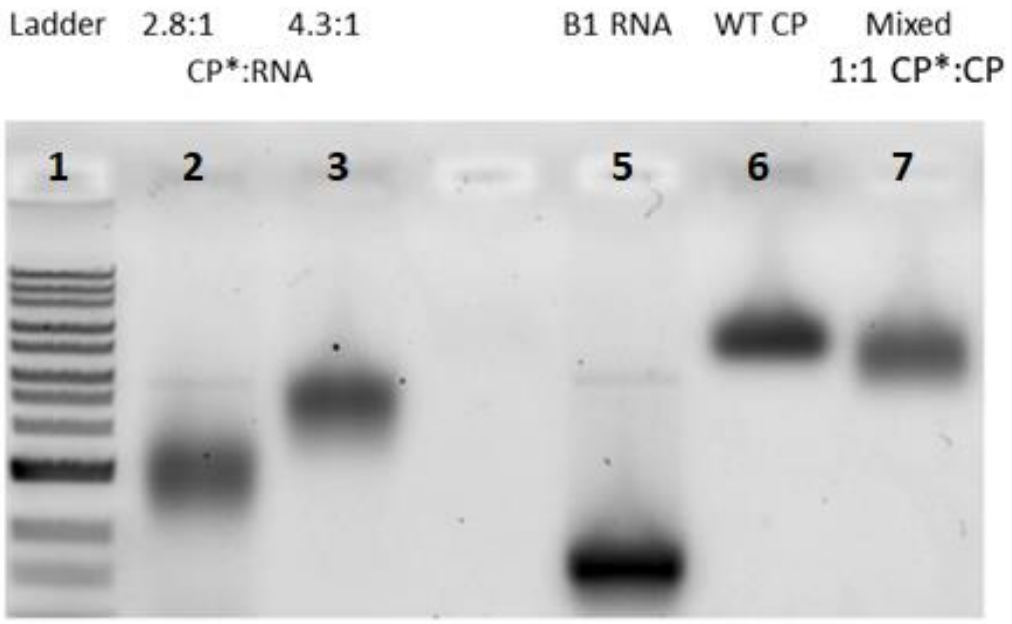

Figure 19: A 1% agarose gel comparing WT CP and cysteine-mutant CP assemblies.

Description of the contents of each line described in text.

Chapter 6: Future Directions and Conclusions

6.1 Future Directions: alterations to the replicon and two-molecule fluorescence co-expression studies

When utilizing the replicon as part of a gene therapy, it may be important to be able to calibrate the activity. As discussed in Chapter 3, dilution of the replicon has an effect on the duration of amplification. Also, the quantity of reporter gene expression from increasing dilutions changes in a non-linear manner. In addition to changing dosages, direct modifications to the GOI replicons can be made for various desired effects. One change to the replicon is re-incorporation of the NoV B2 RNAi-silencing protein by changing the translation promoter region back into the wild-type sequence. It has been demonstrated that in some mammalian cell lines greater replication of NoV can be achieved with the B2 protein than without it[Johnson 2004]. As detailed in Chapter 3. the start of the replicon construct can also be modified by incorporating two extra guanidine (G) nucleotides to the end of the T7 promoter. These extra nucleotides have been shown to increase the yield from *in vitro* transcription about three-fold, but these extra Gs are also incorporated into the beginning of the replicon transcript. We found that replication activity was reduced by about 40% with this alteration, so this can be a means of reducing the activity of the replicon with the added benefit of greater yields from capped transcription.

While the above-described *in vitro* experiments suggest that a two-molecule VLP system could be applied to *in vivo* applications such as intravenous administration of a therapeutic, there are still concerns that need to be addressed. One concern is that a cell might only receive one

type of the two molecules (either the replicon or the GOI-RNA2). By fluorescence-activated cell sorting (FACS), one can compare the number of cells expressing one or both of the two fluorescent proteins. It would also be interesting to see colocalization of the two molecules' fluorescence, suggesting that replication of the RNA2 molecule is occurring. Although this would not be an absolute determination, if most of the fluorescence is co-localized then this would suggest that the cell and/or VLP might have a way of bringing together the particles. A study showed that NoV's RdRp forms functional replication complexes at the outer mitochondrial membrane of cells[Gant 2014]. It is likely that viral RNA or VLPs would want to localize there to coopt host ribosomes and allow for replication by the RdRp.

6.2 Conclusions

All of the work presented throughout these chapters plays some role in the understanding and potential utilization of a combined *Nodamura virus* replicon and CCMV VLP gene delivery system. From the quantitative and qualitative studies of the replicon in BHK 21 cells in Chapter 2, we confirm that the replicon does significantly increase expression of reporter proteins over an equal number of mRNA containing only the reporter gene. From these studies we also observed a non-linear dose dependence of the replicon. At significant dilutions of replicon molecules (40 fold) compared to a typical transfection, the relative light units measured reveals an extended lifetime of replication, and even reaches about half the total luciferase yield.

When packaging the replicon into a CCMV VLP, we observe some interesting trends for its potential as part of a vaccine (Chapter 3). A tandem repeat of ovalbumin's SIINFEKL epitope was inserted into the subgenomic region of RNA1, and this replicon packaged into VLPs was

able to passively be taken up by human dendritic cells during a 24-hour incubation. The replicon-VLPs caused increases in the maturation markers CD 80, CD 86, and MHC II, as well as revealed by qPCR many copies of SIINFEKL-containing RNA. When the VLPs were pre-incubated with anti-CCMV antibodies, the increase of maturation markers and RNA amounts were further increased compared to replicon-VLPs alone. These results demonstrate that CCMV VLPs can be taken up by dendritic cells, where replication then occurs to promote increased production of antigen. Also, if one were to administer repeated dosages of this vaccine, some antibodies decorating the VLPs do not prevent its uptake, or subsequent replication of its RNA cargo.

Length is a consideration when packaging RNA with CCMV CP. If the RNA is overly short or long, the VLP will no longer be the wild type, well-formed individual T=3 capsids. Since many genes are too long to be inserted into the RNA1 of NoV and still be packaged into T=3 single capsids, an alternative is to utilize the RNA2 of NoV. Using 5' and 3' elements of RNA2 known to promote replication by its associated RdRp, we demonstrated that a luciferase gene inserted into this RNA2 molecule (when transfected along with RNA1), yielded greater luciferase activity than the luciferase gene alone.

For some therapeutic applications, specific targeting of the VLP to certain cells may be important. In preparation for this aim, a cysteine-mutant version of CCMV was made. Site-directed mutagenesis of the cDNA clone of the capsid protein-encoding RNA3 was used to allow for a substation of alanine 163 to cysteine. Gold-labeling of the resulting cysteine-mutant CCMV showed that unique surface-exposed cysteines were introduced to form gold-thiol bonds. This cysteine-mutant CP could be disassembled, and undergo assembly in a similar manner to WT

CP. In fact, the two CPs (WT and cysteine-CP) can be assembled in mixtures to control the amounts of labeling sites for subsequent conjugations of targeting ligands to cysteine.

While this work represents a promising platform for gene therapy applications, further work still needs to be done. The *in vivo* T-cell response to the SIINFEKL-Replicon-VLP was statistically significant, but still modest. Further experiments to boost this immune response may involve conjugation of ligands to target the VLPs to dendritic cells, or introduction of an adjuvant gene to help stimulate dendritic cells that have also received the desired antigen.

Bibliography

[Azizgolshani 2013] Azizgolshani O, Garmann RF, Cadena-Nava R, Knobler CM, Gelbart WM. Reconstituted plant viral capsids can release genes to mammalian cells. Virology 2013; 441: 12-17.

[Banerjee 2008] Banerjee M, Johnson JE. Activation, exposure and penetration of virally encoded, membrane-active polypeptides during non-enveloped virus entry. Curr. Protein Pept. Sci. 2008; 9:16–27.

[Ball 1992] Ball LA, Amann JM, Garrett BK. Replication of Nodamura Virus after Transfection of Viral RNA into Mammalian Cells in Culture. Journal of Virology 66.4 (1992): 2326-334.

[Ball 2003] Ball L, Johnson K, Pryce B. Nodavirus-like DNA expression vector and uses therefore. 2003, U.S. Patent 20030108863.

[Biddlecome 2019] Biddlecome A, Habte HH, McGrath KM, Sambanthamoorthy S, Wurm M, Sykora MM, et al. (2019) Delivery of self-amplifying RNA vaccines in in vitro reconstituted virus-like particles. PLoS ONE 14(6): e0215031.

[Brito 2014] Brito LA, Chan M, Shaw CA, Hekele A, Carsillo T, Schaefer M, et al. A cationic nanoemulsion for the delivery of next-generation RNA vaccines. Mol. Ther. 2014; 22: 2118-29.

[Carbone 1992] Carbone FR, Sterry SJ, Butler J, Rodda S, Moore MW. T cell receptor alpha-chain pairing determines the specificity of residue 262 within the Kb-restricted, ovalbumin 257-264 determinant. Int. Immun. 1992; 4: 861-7.

[Cadena-Nava] Cadena-Nava R, Comas-Garcia M, Garmann RF, Rao, ALN, Knobler CM, Gelbart WM. Self- assembly of viral capsid protein and RNA molecules of different sizes: Requirement for a specific high protein/RNA mass ratio. J. Virol. 2012; 86: 12271-82.

[Caspar 1962] Caspar D, Klug A. Physical principles in the construction of regular viruses. Cold Spring Harbor Symp. Quant. Biol. 1962; 27: 1-24.

[Chahal 2016] Chahal JS, Khan OF, Cooper L, McPartlan JS, Tsossie JK, Tilley LD, et al. Dendrimer-RNA nanoparticles generate protective immunity against lethal ebola, H1N1 influenza, and *Toxoplasma gondii* challenges with a single dose. Proc. Nat. Acad. Sci. USA 2016; 113: E4133-42.

[Da Silva 2007] Da Silva DM, Fausch SC, Verbeek JS, Kast WM. Uptake of human papillomavirus virus-like particles by dendritic cells is mediated by Fcγ receptors and contributes to acquisition of T cell immunity. J. Immun. 2007; 178: 7587-97.

[Destito 2007] Destito G, Yeh R, Rae CS, Finn MG, Manchester, M. Folic acid-mediated targeting of cowpea mosaic virus particles to tumor cells. Chem. Biol. 2007; 14: 1152-62.

[Fontaine 2015] Fontaine SD, Reid R, Robinson L, Ashley GW, Santi DV. Long-Term Stabilization of Maleimide–Thiol Conjugates. Bioconjugate Chem. 2015; 26, 1, 145-152

[Gant 2014] Gant, VU Jr, Moreno S, Varela-Ramirez A, Johnson KL. Two Membrane-Associated Regions within the Nodamura Virus RNA-Dependent RNA Polymerase Are Critical for Both Mitochondrial Localization and RNA Replication.. Journal of Virology 88.11 (2014): 5912–5926.

[Garmann 2014a] Garmann RF, Comas-Garcia M, Gopal A, Knobler CM, Gelbart WM. The assembly pathway of an icosahedral single-stranded RNA virus depends on the strength of inter-subunit attractions. J. Mol. Biol. 2014 426: 1050-60.

[Garmann 2014b] Garmann RF, Comas-Garcia M, Koay MST, Cornelissen JLM, Knobler CM, Gelbart WM. Role of electrostatics in the assembly pathway of a single-stranded RNA virus. J. Virol. 2014; 88: 10472-9.

[Garmann 2016] Garmann RF, Comas-Garcia M, Knobler CM, Gelbart WM. Physical principles in the self-assembly of a simple spherical virus. Acc. Chem. Res. 2016; 49: 48-55.

[Geall 2012] Geall AJ, Verma A, Otten GR, Shaw CA, Hekele A, Banerjee K, et al. Nonviral delivery of self-amplifying RNA vaccines. Proc. Nat. Acad. Sci. USA 2012; 109: 14604-9.

[Gitlin 2014] Gitlin L, Hagai T, LaBarbera A, Solovey M, Andino R. Rapid evolution of virus sequences in intrinsically disordered protein regions. PLOS Pathogens 2014; 10: e1004529.

[Hovlid 2012] Hovlid ML, Steinmetz NF, Laufer B, Lau JL, Kuzelka J, Wang Q, et al. Guiding plant virus particles to integrin-displaying cells. Nanoscale 2012; 4: 3698-705.

[Islam 2015] Islam MA, Reesor EKG, Xu Y, Zope HR, Zetter BR, Shi J. Biomaterials for mRNA Delivery. Biomaterials science 3.12 (2015): 1519–1533.

[Johnson 2003] Johnson K, Duane Price B, Ball LA. Recovery of infectivity from cDNA clones of nodamura virus and identification of small nonstructural proteins. Virology 2003; 305: 436–51.

[Kemnade 2014] Kemnade JO, Seethammagari M, Collinson-Pautz M, Kaur H, Spencer DM, McCormick AA. Tobacco mosaic virus efficiently targets DC uptake, activation and antigen-specific T cell responses *in vivo*. Vaccine 2014; 32: 4228-33.

[Kovacs 2007] Kovacs EW, Hooker JM, Romanini DW, Holder PG, Berry KE, Francis MB. Dual-surface-modified bacteriophage MS2 as an ideal scaffold for a viral capsid-based drug delivery system. Bioconjugate Chem. 2007; 18: 1140-7.

[Kwong 1998] Kwong PD, Wyatt R, Robinson J, Sweet RW, Sodroski J, Hendrickson WA. Structure of an HIV gp120 envelope glycoprotein in complex with the CD4 receptor and a neutralizing human antibody. Nature 1998; 393, 648-659

[Lam 2017] Lam P, Steinmetz NF. Plant viral and bacteriophage delivery of nucleic acid therapeutics. WIRES Nanomed. and Nanobiotechnol. 2017; 10: e1487. doi: 10.1002/wnan.1487

[Maruggi 2019] Maruggi G, Zhang C, Li J, Ulmer JB, Yu D. mRNA as a Transformative Technology for Vaccine Development to Control Infectious Diseases. Mol. Therapy 2019; 27: 1-16

[Owens 2012] Owens, Flores, Di Serio, Francesco, Li, Shifan, Pallás, Vicente, Randles, Sano, Vidalakis. Virus Taxonomy: Ninth Report of the International Committee on Taxonomy of Viruses. 2012

[Rohovie 2017] Rohovie M, Nagasawa M, Swartz JR. Virus-like particles: Next-generation nanoparticles for targeted therapeutic delivery. Bioeng. Transl. Med. 2017; 2: 43-57.

[Rosskopf 2010] Rosskopf JJ, Upton, III JH, Rodarte L, Romero TA, Leung MY, Taufer M, et al. A 3′ terminal stem-loop structure in *Nodamura virus* RNA2 forms an essential *cis*-acting signal for RNA replication. Virus Res. 2010 Jun; 150(1-2): 12-21

[Schoggins 2011] Schoggins JW, Wilson SJ, Panis M, Murphy MY, Jones CT, Bieniasz P, et al. A diverse range of gene products are effectors of the type I interferon antiviral response. Nature 2011; 472: 481-5.

[Schott 2010] Schott J, Stoecklin G. Networks controlling mRNA decay in the immune system. WIREs RNA 2010; 1: 432-6.

[Speir 1995] Speir JA, Mushi S, Wang G, Baker TS, Johnson JE. Structures of the native and swollen forms of cowpea chlorotic mosaic virus by X-ray crystallography and cryo-electron microscopy. Structure 1995; 15: 63-78.

[Stephanopoulos 2010] Stephanopoulos N, Tong GJ, Hsiao SC, Francis MB. Dual-surface-modified virus capsids for targeted delivery of photodynamic agents to cancer cells. ACS Nano 2010; 4: 6014-20.

[Sullivan 2005] Sullivan CA, Ganem D. A Virus-encoded inhibitor that blocks RNA interference in mammalian cells. J. Virol. 2005 Jun; 79(12): 7371-9.

[Tesh 1980] Tesh RB. Infectivity and Pathogenicity of Nodamura Virus for Mosquitoes. Journal of General Virology. 1980: 48. 177-182. 10.1099/0022-1317-48-1-177.